Cardiovascular Magnetic Resonance in Non-Ischemic Myocardial Inflammation: *JACC* Scientific Expert Panel

Vanessa M. Ferreira, MD DPhil[1]; Jeanette Schulz-Menger, MD[2]; Godtfred Holmvang, MD[3]; Christopher M. Kramer, MD[4]; Iacopo Carbone, MD[5]; Udo Sechtem, MD[6]; Ingrid Kindermann, MD[7], Matthias Gutberlet, MD[8]; Leslie T. Cooper, MD[9]; Peter Liu, MD[10] Matthias G. Friedrich, MD[11,12]

[1]University of Oxford Centre for Clinical Magnetic Resonance Research, John Radcliffe Hospital, Oxford, United Kingdom; [2]: Department of Cardiology, Universitätsmedizin Charité, Helios-Klinikum Berlin, Germany; [3]: Division of Cardiology and Department of Radiology, Massachusetts General Hospital, Boston, USA; [4]: Department of Cardiology, University of Virginia, Charlottesville, VA, USA; [5]: Department of Radiology, Sapienza, University of Rome, Italy; [6]: Department of Cardiology, Robert-Bosch-Krankenhaus, Stuttgart, Germany; [7]: Department of Internal Medicine III, Saarland University Medical Center, Homburg/Saar, Germany; [8]: Department of Diagnostic and Interventional Radiology, University of Leipzig, Heart Center, Leipzig, Germany; [9]: Department of Cardiology, Mayo Clinic, Rochester, MD, USA; [10]: Ottawa Heart Institute, Ottawa, ON, Canada; [11]: Heidelberg University Hospital, Heidelberg, Germany; [12]: Departments of Cardiology and Diagnostic Radiology, McGill University Health Centre, Montreal, Canada

Short title: 2018 Update of CMR Criteria for Myocardial Inflammation

Acknowledgments: The authors acknowledge the tremendous help from Dr. Stefan Piechnik, Associate Professor of Biomedical Imaging, University of Oxford Centre for Clinical Magnetic Resonance Research, for his extensive review and systematic statistical analysis. The authors also thank Ebe Schaub MD, University Hospital Heidelberg, for the help with preparing the example images for the central illustration. Dr. Ferreira acknowledges support from the National Institute of Health Research Biomedical Research Centre, Oxford, and the British Heart Foundation Centre of Research Excellence, Oxford. Special thanks also go to Dr. Iacopo Carbone, for his hospitality at the meeting venue in Italy.

Disclosures: Dr. Friedrich is board member, adviser and shareholder of Circle Cardiovascular Imaging. Dr. Kramer is a consultant for Bayer Healthcare. Dr. Schulz-Menger is a consultant for Bayer Healthcare and Siemens Healthineers. Dr. Gutberlet received moderate speaker honorarium from Bayer, Bracco, Siemens and Philips. No other author has relevant disclosures.

Corresponding Author:
Matthias G. Friedrich, MD
Departments of Medicine and Diagnostic Radiology, McGill University
Professor of Medicine, Department of Medicine, Heidelberg University
Department of Radiology, Université de Montréal
Departments of Cardiac Sciences and Radiology, University of Calgary
McGill University Health Centre
1001 Decarie Boulevard
Montreal, Quebec H4A 3J1 Canada
Telephone: 514-934-1934,38106
Fax: 514-843-2813
E-mail: mgwfriedrich@gmail.com
Twitter: @mgwfriedrich | @cusm_muhc

Abstract
This *JACC* Scientific Expert Panel provides consensus recommendations for an update of the cardiovascular magnetic resonance (CMR) diagnostic criteria for myocardial inflammation in patients with suspected acute or active myocardial inflammation (Lake Louise Criteria), that include options to use parametric mapping techniques. The authors propose that CMR provides strong imaging evidence for myocardial inflammation, if the CMR scan demonstrates the combination of myocardial edema with other CMR markers of inflammatory myocardial injury. This is based on at least one T2-based criterion (a global or regional increase of myocardial T2 relaxation time or an increased signal intensity in T2-weighted CMR images), with at least one T1-based criterion (increased myocardial T1, increased extracellular volume, or increased signal intensity in Late Gadolinium Enhancement images). The update is expected to further improve the diagnostic accuracy of CMR in detecting myocardial inflammation.

Keywords: Cardiovascular Magnetic Resonance, Myocarditis, Myocardial Inflammation

Condensed Abstract
This *JACC* Scientific Expert Panel provides consensus recommendations for an update of the cardiovascular magnetic resonance (CMR) diagnostic criteria for myocardial inflammation in patients with suspected acute or active myocardial inflammation (Lake Louise Criteria), including options to use novel parametric mapping techniques. The authors propose that CMR provides strong evidence for myocardial inflammation if the CMR scan demonstrates the combination of CMR markers for myocardial edema with other CMR markers of inflammatory myocardial injury. The updated Lake Louise Criteria are based on the combination of at least one T2-based criterion, with at least one T1-based criterion; these can include T1-, T2- and ECV-mapping.

Abbreviations
AUC - area-under-the-curve
AUC* - estimated area-under-the-curve
CMR - Cardiovascular magnetic resonance
ECG - Electrocardiogram
ECV - Extracellular volume
EGE - Early gadolinium enhancement
EMB - Endomyocardial biopsy
GBCA - Gadolinium-based contrast agent
LLC - Lake Louise Criteria
LGE - Late gadolinium enhancement
SI - signal intensity
SNR - signal-to-noise ratio
SSFP - Steady-state free precession
STIR - Short-tau inversion recovery

Purpose of an Update of the Lake Louise Criteria

In 2009, the Consensus Criteria for Cardiovascular Magnetic Resonance (CMR) in Myocardial Inflammation ("Lake Louise Criteria") were published (1). These criteria proposed three diagnostic targets in the myocardial tissue—edema, hyperemia and necrosis/scar—derived from signal intensity assessment in T2-weighted, early gadolinium enhancement (EGE) and late gadolinium enhancement (LGE) CMR images. Based on published data, it was suggested to assume a high likelihood of acute myocarditis (inflammation), if the CMR images indicated that 2 out of 4 three criteria are positive (1). Based on a limited number of published studies at that time, the diagnostic accuracy had been estimated at 78%, with a sensitivity of 67% and a specificity of 91%. Since then, the Lake Louise Criteria have been used extensively in both clinical and research settings. While some of the criteria and methods for their evaluation have been subject of discussion, these numbers were largely confirmed by subsequent studies, including in vivo validation. These were summarized by recent meta-analyses evaluating the Lake Louise Criteria to identify acute myocarditis, with one reporting a pooled diagnostic accuracy of 83% (sensitivity 80%; specificity 87%) (2) and another reporting similar diagnostic accuracy based on 7 studies, with summary sensitivity of 78%, specificity of 88% and area-under-the-curve of 83% (3). CMR has informed clinical decision-making in many thousands of patients, and can avoid invasive procedures, such as coronary angiography and endomyocardial biopsies (3).

CMR tissue characterization using signal intensities only, however, have some shortcomings. When the inflammatory processes become increasingly diffuse throughout the myocardium (more common after the first several days as myocarditis transitions from acute to sub-acute), T2 and EGE signal intensity may also become progressively more homogeneous, to

the point where discrete lesions may no longer be easily detected on qualitative review. While diffuse changes could still be identified as an increased global signal intensity ratio, normalized against reference regions in skeletal muscle, coexisting skeletal muscle inflammation may lead to false negative results (4,5). Furthermore, other non-inflammatory conditions, such as infiltrative cardiomyopathies, may also increase the myocardial extracellular space and gadolinium uptake.

Technical advances, specifically the development of pixel-wise mapping of T1 and T2 relaxation times, have led to multiple studies reporting their clinical potential in patients with suspected myocardial inflammation. It is, therefore, timely to review the current published evidence, and revise the Lake Louise Criteria accordingly.

Background

Myocardial inflammation can be caused by the immune response to viruses, auto-immune disease, ischemic injury, or toxic agents (6,7), and is an important underlying etiology for chest pain and other symptoms. The cascade of pathophysiologic mechanisms is complex, and therapeutic options, especially for viral myocarditis, are the subject of intense research (8). In the clinical setting of acute chest pain and cardiomyopathy, a diagnosis of myocardial inflammation by CMR imaging or biopsy can significantly impact prognosis and management (9,10). Imaging in the acute setting can provide valuable clues to the etiology of the presenting symptom(s), especially differentiating ischemic from non-ischemic etiologies, and diagnosing valvular and pericardial disease (11). The current European Society of Cardiology (ESC) position statement (12) and American Heart Association (AHA) scientific statement on the management of myocarditis (13) consider CMR useful for the evaluation of suspected myocarditis. Although definitive confirmation of specific etiologies of myocarditis (e.g. viral) requires histopathologic and molecular biological evaluation of myocardial tissue samples, CMR has a unique role in

both the non-invasive detection and exclusion of myocardial inflammation. This is especially relevant in cases involving the epicardium, pericardium or other regions not accessible to endomyocardial biopsy (EMB), as well as assessment of alternate diagnoses responsible for the acute presentation. CMR is able to provide a non-invasive, biopsy-like approach to verify pathognomonic imaging features of myocardial inflammation, and the current ESC guidelines on acute and chronic heart failure include a class I indication for CMR for the assessment of myocarditis and storage diseases (14).

CMR characteristics of myocardial inflammation may not only aid in the diagnosis of myocarditis, but also provide information on prognosis. While inflammatory syndromes often evolve over days to weeks and then resolve, they may also transition into chronic dilated cardiomyopathy. The course of myocardial inflammation limits the optimal sensitivity for diagnostic imaging to a few weeks from presentation (15). Within this window, however, CMR can identify useful features, which may also predict outcome (16). In acute cases, myocardial edema without LGE on CMR has been associated with improved recovery and outcomes (17). In adults requiring ventricular assist device support, myocarditis is one of the best predictors of a bridge to recovery (18). In cases of acute viral heart disease, the CMR pattern of myocardial inflammation may vary, and findings on edema-sensitive T2-weighted images correlate with the presence of viral genomes in the blood (19). CMR provides incremental data to EMB that may aid disease management (20). Thus, CMR has evolved to become a key evaluation tool in patients with suspected myocardial inflammation.

Clinical context of patients with suspected myocardial inflammation

Clinical presentation

Patients with myocarditis may present with a broad spectrum of symptoms due to the various cardiac structures involved in the inflammatory process (cardiomyocytes, interstitium, endothelium and pericardium) (6,11). These symptoms range from mild discomfort caused by palpitations or non-specific chest pain to more dramatic clinical features similar to acute myocardial infarction, including angina pectoris, ST-segment elevations on ECG, as well as elevated markers of myocyte necrosis (troponin, creatine kinase). Acute congestive heart failure, with or without cardiogenic shock, or progressive chronic heart failure can occur. Furthermore, supraventricular and ventricular tachyarrhythmias, as well as bradyarrhythmias and intraventricular conduction delays, are common in these patients (21).

The acute phase of viral myocarditis lasts only for a few (one to three) days. It is characterized by pathognomonic myocyte necrosis induced by virus replication after infection. The resulting exposure of intracellular antigens may lead to the activation of a cascade of humoral and cellular immunologic processes aimed to eliminate the virus in the myocardium. In some patients, this immunological reaction may persist for several weeks or months, independently of myocardial viral genome detection, resulting in chronic post-infectious autoimmune myocarditis (6,9).

Clinical work-up of acute myocardial inflammation

In suspected acute myocardial injury, acute coronary syndrome and stress-induced cardiomyopathy should be excluded, especially in patients with chest pain, heart failure or new arrhythmia. The clinical presentation and symptoms of a patient with acute myocardial inflammation may provide clues to the etiology of the disease, such as recent exposure to toxic or allergenic agents. Regarding viral myocarditis, the position statement of the ESC Working Group on Myocardial and Pericardial Diseases (2013) proposed new diagnostic criteria, which

are intended to reinforce the diagnosis (12). According to this statement, myocarditis is suspected if one or more symptoms, such as chest pain, dyspnea, fatigue, palpitations, or syncope, and at least one of the diagnostic (including CMR) criteria in **Table 1**, are present. Most of the recommendations were based on assessment of viral myocarditis, but can be extended to myocardial inflammation of other etiologies.

Other tests for myocardial inflammation

Several *laboratory tests* are recommended in patients with clinically suspected myocarditis (12), although serum markers of inflammation are not very sensitive (22), and routine viral serology testing is not very specific (23).

Standard *12-lead ECG* may show ST-segment elevation, T-wave changes, conduction abnormalities as well as arrhythmia, but are neither specific nor sensitive enough to allow a definitive diagnosis (12, 21) or rule out inflammatory heart disease (24) as a stand-alone diagnostic test.

Echocardiography may help to rule out other causes of heart failure, such as valvular disease, congenital heart disease or other cardiomyopathies, and to monitor significant changes of wall motion (12, 25). In case of acute myocardial inflammation, echocardiography may show normal or altered ventricular dimensions, impaired function and, less frequently, increased wall thickness due to edema, whereas chronic myocarditis may present with ventricular dilatation and regional or global hypokinesis. These changes are non-specific but may be useful for longitudinal studies. Echocardiography may also help visualize pericardial effusion or intracavitary thrombi (6).

Recently, *positron emission tomography* (PET) has shown good agreement with CMR criteria of inflammation (26), although its clinical use remains uncommon due to limited

availability and cost. **Table 1** lists the currently used non-invasive diagnostic procedures and potential findings in myocarditis (12).

Endomyocardial biopsy (EMB) is still the gold standard for identifying the specific etiology of myocarditis, and uses histopathological, immunohistochemical and molecular biological criteria. In the hands of experienced operators, EMB has a low complication rate of <1% (27). According to the recommendations of the American Heart Association, the American College of Cardiology and the European Society of Cardiology, the indication for EMB should be considered for patients with acute (<2 weeks), severe new-onset heart failure with hemodynamic compromise, as well as new-onset heart failure (between 2 weeks to 3 months) with a dilated left ventricle and new ventricular arrhythmias, AV-block II-III, or failure to respond to medical therapy and usual care within 1 to 2 weeks (Class I Recommendation, Level of Evidence B) (28). For patients with an infarction-like presentation, the ESC Working Group statement recommends EMB after the exclusion of coronary heart disease (12), whereas more recent heart failure guidelines grant CMR a class I recommendation to identify myocarditis in patients with suspected or established heart failure (14). EMB should also be considered in patients with persistently elevated troponin values and progressive cardiac dysfunction despite maximal heart failure therapy. The pre-procedural localization of inflammatory changes in CMR images may reduce sampling errors, and improve therapeutic decision-making and prognostication (29-31).

Diagnostic targets of CMR in myocardial inflammation

CMR imaging sequences are sensitive to the tissue changes that occur during myocardial inflammation, regardless of etiology. These pathophysiologic changes include: dilatation of the myocardial vascular bed with hyperemia; increased vascular permeability/capillary leak; edema

(both intracellular and interstitial); myocyte injury with loss of cell membrane integrity; myocyte necrosis; accumulation of debris in the extracellular space; infiltration of inflammatory cells/macrophages; and, ultimately, collagen deposition with formation of interstitial fibrosis and scar. The magnitude and spatial extent of these changes depend on the severity of the inflammation. While there may be distinct types of clinical presentations of myocardial inflammation (e.g., infarct-like or heart-failure-like), ultimately, the determinants of clinical presentation in an individual are multi-factorial, including the etiology of myocarditis, the load of the offending agent, degree of severity and extent of the inflammatory process, as well as host factors, such as the immune response and symptoms experienced. Accordingly, CMR only detects the presence or absence of signal changes that are the result of underlying tissue inflammation, but in most cases does not define the etiologies for the myocardial inflammation that is observed. However, CMR may be useful as a phenotypic tool to examine for any systematic differences or characteristics between patient subgroups based on presentation features.

Myocardial Edema

Tissue edema, mediated by bradykinin, serotonin, and prostaglandins, is a hallmark of inflammation in all soft tissues. Clinically-relevant inflammation inevitably includes edema of the affected tissue. On CMR, the increased tissue water content (edema) causes prolongation of both T1 and, especially, T2 relaxation times in the myocardium. Several CMR approaches can therefore be used to detect edema. In T2-weighted (T2-w) images, edema appears as regional or global signal hyperintensity. T2 mapping allows for the direct measurement of the water-induced prolongation of myocardial T2 relaxation time (32). Edema also leads to an increase of myocardial T1 relaxation time (33), although the increase of T1 is less specific for active

inflammation, as it can also be seen in areas of fibrosis where free water may accumulate (34). It is important to note that myocardial edema can also occur due to venous congestion as in acute decompensated heart failure (35).

Hyperemia and Capillary Leak

In addition to the increased free water content of tissue, inflammation also leads to hyperemia, increased vascular permeability and a net expansion of the extracellular space. CMR techniques to target these changes include T1-weighted (T1-w) spin echo images acquired pre- and early post-administration of an extracellular gadolinium-based contrast agent (GBCA) (36). Because Gadolinium in its ligated form is an extracellular contrast agent, it is believed that the increased volume of distribution available for GBCA leads to greater contrast enhancement compared to non-inflamed myocardium, although it ultimately remains unclear whether these methods can specifically reflect hyperemia or are just markers of an expansion of the extracellular space.

Necrosis and fibrosis

If the inflammation is severe enough to cause myocyte injury, followed by necrosis, fibrosis and scarring, there is a further substantial increase in the volume of distribution available for GBCA, as the contrast agent gains access to the intracellular space of myocytes that are injured or no longer viable. Studies using Late Gadolinium Enhancement (LGE) images have identified common patterns of the regional distribution of such injuries. These images have become well established as an invaluable tool for identifying the "signature pattern" of non-ischemic inflammatory injury, and to differentiate it from other types of myocardial pathology. Myocarditis lesions tend to be patchy, subepicardial (in contrast to ischemic lesions which involve the subendocardium), mid-wall, and favor the basal to mid inferolateral walls.

Exceptions do occur, and in severe inflammation, the high signal intensity regions may extend fully through to the subendocardium. Myocardial inflammation due to hypereosinophilia syndromes typically shows a circumferential subendocardial LGE pattern which does not localize to any specific coronary territory (37).

Functional abnormalities

Dysfunction ("functio laesa") is considered a feature of inflammation. Dysfunction in myocarditis, however, can be focal, and the surrounding myocardium may compensate by an increase in contractility, which lets the tethered, affected myocardium appear inconspicuous. Furthermore, the predominantly subepicardial involvement of more severe injury may leave the contraction of other myocardial layers unaffected. Wall motion abnormalities can be the due to other conditions, and ejection fraction may be preserved even in the presence of elevated T2 or LGE abnormalities. Thus, ventricular dysfunction is not a very sensitive nor specific finding for myocardial inflammation. However, if there is evidence for a recent, rapid decline in ventricular function, the list of other non-inflammatory etiologies is relatively short and may be easy to exclude (e.g., tachycardia-mediated, chemotherapy, alcohol, thyroid disorders); an ischemic injury can usually be excluded by the LGE images. Myocardial strain mapping may increase sensitivity for detection of subtle wall motion abnormalities but is unlikely to add specificity for myocardial inflammation. Overall, functional abnormalities are considered a supportive criterion for myocardial inflammation.

Pericardial abnormalities

Myocardial inflammation may be associated with pericardial involvement, and vice versa. The presence of pericardial effusion alone does not prove pericarditis, as this may simply reflect coexisting heart failure. Active pericardial inflammation, however, becomes likely if there is

associated thickening of the pericardial layers in high-resolution fast spin echo T1 images, hyperintensity of the pericardium on T2-w images, T2- or T1-mapping, and abnormal pericardial late gadolinium enhancement (38). Pericardial abnormalities indicating inflammation are considered a supportive criterion.

Novel CMR mapping techniques for detecting myocardial inflammation

Recently, there has been substantial progress in the development of CMR mapping techniques, allowing efficient measurement of myocardial T1 and T2 relaxation times in patients with acute myocardial inflammation (5,39). T1 and T2 relaxation times are magnetic properties of tissue that are influenced by intrinsic tissue characteristics, their extrinsic environment, and method of measurement, including hardware and software platforms. Each tissue type has a specific normal range of T1 and T2 relaxation times (dependent on the method of measurement), deviation from which may indicate disease or a change in physiology. T1 and T2 relaxation times are calculated on a pixel-by-pixel basis and displayed as maps; global or regional myocardial T1 or T2 values can then be obtained. The extracellular volume (ECV) may also be estimated in myocarditis using T1 maps acquired pre- and post-administration of GBCA and adjusting for the hematocrit value (40). Beyond providing global T1, T2 or ECV values, advanced image analysis may be required, and is recommended as necessary, for identifying regional abnormalities and non-ischemic patterns of acute myocardial injury compatible with myocarditis, based on validated thresholds, and potentially pixel heterogeneity. (5,39,41-43).

Cardiac mapping is a rapidly evolving field and, thus, standardized methods and protocols are still being established. For T1-mapping, the most widely used approaches include inversion-recovery (e.g., MOLLI, ShMOLLI), saturation-recovery (SASHA), or hybrid methods (44). T2-mapping techniques commonly employ gradient and spin echo using multi-echo

readouts (39,45,46). As mapping is sensitive to the hardware and software used, local validation should be performed and benchmarked against established norms for a chosen method (44). Significant deviation from known norms for a method should prompt investigation, so that any issues with method implementation or application may be addressed. Validated diagnostic thresholds are likely to be method-specific. It is important to note that the use of thresholds (whether semi-quantitative or quantitative) is always a trade-off between sensitivity and specificity in detecting a disease entity. The diagnostic performance of CMR for detecting myocarditis, whether using conventional methods or newer mapping techniques, depends on multiple factors, including the method's metrological properties, hardware and software platforms, end-user adherence to prescribed protocols and experience, the quality of the images, and standardization. Further recommendations on the set-up and use of parametric mapping methods may be found in consensus statements published in conjunction with scientific bodies such as the Society for Cardiovascular Magnetic Resonance (SCMR) and the European Association of Cardiovascular Imaging (EACVI), which may release regular updates as the field evolves (44,47). The Consensus Group looks forward to more data becoming available regarding the possibility of using a standardized phantom to relate T1, ECV, and T2 measurements of normal ranges and diagnostic thresholds, across different MRI system vendors, pulse sequences and imaging sites.

Mapping of T1 and T2 for the Detection of Myocardial Inflammation

Inflamed myocardium exhibits higher values of T1, T2, and ECV, all of which can be quantified directly without relying on relative signal intensity changes, circumventing the limitations of semi-quantitative tissue characterization techniques. Multiple studies have described excellent sensitivity, specificity and diagnostic accuracy achieved by mapping

techniques for the CMR evaluation of suspected myocarditis. **Table 2** and the **Online Appendix** provide pooled data from currently available clinical studies on the diagnostic performance of the original Lake Louise Criteria I and novel mapping techniques (2).

For example, Ferreira et al. reported an 89% diagnostic accuracy of native T1-mapping alone in patients hospitalized for acute myocarditis studied within 14 days of symptom onset (42). In the MyoRacer myocarditis trial (which used EMB as the diagnostic standard), native T1-mapping yielded the highest diagnostic accuracy (81%) of all the CMR parameters tested in the patient group with acute symptoms ($\leq$14 days from symptom onset to hospital admission), but accuracy dropped to 45% in differentiation from the chronic group (studied >14 days after onset of symptoms) (15). The MyoRacer trial included patients with chronic heart failure, as long as they had evidence for recent systemic viral disease. Studies in suspected chronic myocarditis are more likely to also include patients with heart failure due to other non-inflammatory forms of heart disease known to be associated with prolongation of myocardial T1 values (and ECV expansion). These may include infiltrative cardiomyopathies, such as amyloidosis, or diffuse myocardial fibrosis from any of multiple causes, resulting in reduced specificity for acute inflammation (a similar limitation described for the EGE technique).

There is evidence that T2-mapping may be more specific to acute inflammation compared to T1-mapping, which is also sensitive to detection of water in more chronic settings, such as in areas of scarring, ischemia or other causes of expanded extracellular space, and this deserves further investigation. In the MyoRacer trial, T2-mapping was the only CMR parameter with acceptable diagnostic accuracy (73%) for detecting biopsy-proven myocarditis in patients with chronic (>14 days) symptoms (15). This underlines the complementary nature of T1- and T2-based measurements, and the need to include both in the CMR protocol based on current

evidence. T1 and T2 elevations are most marked during early, acute inflammation (48). As acute inflammation and tissue edema subside, the associated prolongation of T1 and T2 relaxation times also diminishes, eventually leaving only sequelae in the form of residual subepicardial or mid-wall fibrosis/scar, typically seen on LGE images. Both T1 and T2 are sensitive to changes in tissue water, but method design, MRI parameters, including magnetization transfer effects (49), may highlight certain MR signals in certain disease settings. Larger and longer-term studies on mapping techniques are needed to determine their clinical impact on patients in myocarditis.

Evidence of Clinical Utility of CMR in Patients with Suspected Acute Myocardial Inflammation

The original Lake Louise Criteria I provide a good overall diagnostic performance (**Table 2; Figure 1**), and thus should remain in use in centers which have good experience with their application. Any diagnostic criteria should include diagnostic targets associated with inflammation, such as (a) myocardial edema, (b) global hyperemia and capillary leak (increased vascular and extravascular space), and (c) focal necrosis/fibrosis/scar.

Myocardial edema (T2-weighted imaging)

Black-blood spin echo sequences (typically as a Short-Tau Inversion Recovery sequence, STIR) exploit T2 and T1 changes in myocardial edema (50,51), and generally have a very good accuracy (52). Triple inversion recovery (IR) techniques typically allow for more homogeneous fat suppression compared to dual IR techniques with chemical fat saturation, but this comes with a signal-to-noise penalty. T2-prepared SSFP-based bright blood sequences appear to be an alternative, albeit less robust for detecting global myocardial edema (33). Systolic images of regular SSFP cine sequences can also be helpful in detecting regional signal hyper-intensity in edematous areas (53). When no localized T2 hyper-intensity is visible in the images to allow

identification of focal inflammatory lesions, the increase in global T2 signal can still be detected by an increased ratio of signal intensity in the myocardium relative to a reference region in skeletal muscle within the same image (with a ratio of ≥2.0 considered abnormal) (1). The ratio may vary slightly between MR systems, and also depends on the use of the integrated body coil. A recent study found that the presence of transmural edema, as visualized in T2-weighted CMR images, was the only independent predictor of T wave inversions observed on the ECG (odds ratio 9.96 [95% CI 2.71–36.6]) (54). However, the technique is often limited by an inherently low signal-to-noise (SNR) ratio, susceptibility to arrhythmia and motion, and inconsistent image quality (55,56). Data indicate that the main value of T2-weighted imaging, when the image quality is good, lies in its ability to rule out significant myocarditis (negative predictive value of 80%) (2). Of note, the involvement of skeletal muscle in a systemic inflammatory disease may yield false negative results for the ratio (5,57).

Hyperemia and Capillary Leakage (Early Gadolinium Enhancement)

The increased uptake of an interstitial contrast agent can be visualized and semi-quantitatively assessed in T1-weighted CMR images before and early after GBCA administration. The uptake can be quantified using the myocardial signal intensity enhancement relative to a skeletal muscle reference region in the same image (with a ratio of ≥4.0 consistent with inflammation). This has been referred to as the Early Gadolinium Enhancement Ratio (EGEr). Alternatively, the contrast-media induced relative myocardial signal intensity increase (cut-off 45%) can be used. The value of the ratio may vary slightly among different MR systems and settings. EGE is considered useful by many experts; yet, in most centers, it is not routinely used due to difficulties with the consistency of image quality. Recent data indicated that removing EGE from the original Lake Louise criteria does not significantly reduce diagnostic

accuracy for myocarditis, although the positive likelihood ratio may be slightly lowered (58). EGE has been considered useful as a third CMR technique, especially in cases of non-diagnostic image quality of either T2-weighted or LGE imaging. Thus, centers experienced in the use of EGE and without access to myocardial mapping sequences may prefer to use the original Lake Louise Criteria that include EGE.

Myocardial necrosis and fibrosis (Late Gadolinium Enhancement)

If inflammation is severe enough, it will cause cell death, which leads to necrosis and an additional compartment for GBCA accumulation. Following a delay after injection (typically about 10 minutes) to allow time for contrast to wash out of non-injured myocardium, there will be a GBCA concentration differential between regions with more severe versus less intense or absent myocyte damage. This allows visualization of the necrosis and scarring due to the differential enhancement. Inversion-recovery prepared gradient echo pulse sequences are used to produce LGE images, to visualize the lesions by nulling the signal intensity of reference normal myocardium to zero.

As the acute inflammatory lesions (necrosis) transition to fibrosis and scar-formation, the markers of active inflammation gradually resolve, while the regional LGE usually persists on follow-up imaging, as GBCA will now distribute into the extracellular space of the collagen matrix, in a manner similar to the evolution of an ischemic scar. The spatial extent LGE lesions shrinks over time (59) and their signal intensity tend to increase, as the tissue swelling from edema subsides and the scar contracts, but despite these changes over time, LGE imaging alone cannot, by itself, reliably differentiate between a recent and remote episode of myocarditis.

LGE is widely used for detecting regional replacement fibrosis or other forms of irreversible injury, infiltration or fibrous degeneration. In acute, “infarct-like” myocarditis, its

sensitivity is high (60). LGE used in isolation is not recommended, however, as it is not very sensitive in very mild cases, and is not specific for active/acute inflammation, especially in cases of predominantly global edema. It should be emphasized that, while LGE specifically detects expanded extracellular space caused by the disease process (such as myocyte necrosis, fibrosis, or edema), it does not signal inflammation itself.

It is important to note that most clinical studies have used clinical criteria to define myocardial inflammation. EMB studies, however, may also suffer from selection bias due to the narrow range of clinical indications for EMB in more severe and chronic cases, and the need for an invasive procedure. In the absence of the true gold standard, which is the whole-heart specimen for histopathologic examination for myocardial inflammation, limitations to commonly-used diagnostic tools would need to be acknowledged and accepted for pragmatic clinical practice.

Evidence for Novel CMR Mapping Techniques (T2-mapping, T1-mapping and ECV)

T2-mapping

Experimental and clinical studies have shown that T2 mapping can identify acute myocardial edema, with very good diagnostic accuracy when compared with traditional T2-weighted imaging (15,39,61,62). Specific advantages of mapping, such as higher SNR, shorter breath-holds with fewer breathing motion artifacts, and direct quantification, all improve intra- and interobserver variability and diagnostic confidence. The sensitivity of T2-weighted imaging in chronic stages of myocardial inflammation has been questioned (20,63,64), although patient selection and definition of chronic myocarditis may have introduced bias. Recently published data, on the other hand, demonstrated an advantage of T2 mapping over T2-weighted imaging in patients with biopsy-proven active chronic myocarditis (15). Like T2-weighted imaging, T2

mapping may be particularly useful in ruling out active inflammation (sensitivity of 89% (52)). Recent data confirm the ability of T2 mapping to discriminate active from healed myocarditis (65). Because of its specificity for acute processes, the presence of edema in the absence of acute ischemic injury is considered an essential criterion for inflammation.

Native T1-mapping

As discussed, T1 relaxation time is highly sensitive to detecting both acute and chronic forms of an increased free water content within the myocardium, and thus, may be best paired with T2-based imaging to augment the specificity for active inflammation and edema in myocarditis (42). Additionally, in acute myocardial inflammation, vasodilation, hyperemia, and increased interstitial space also increase native T1 (42,66). Native T1 is sensitive to intra- and extra-cellular changes in free water content.

A number of studies have shown that T1 is increased in acute (5,42,67,68) and chronic (52,65,68) myocarditis. While some data suggested that native T1 may allow for differentiating different stages of myocarditis (68), there is considerable overlap between results found in acute and convalescent myocarditis, as areas of chronic regional or diffuse fibrosis also increase T1 (69,70). Accordingly, a recent study indicated that T1 alone may not be able to discriminate acute from chronic disease (52). Thus, an increased myocardial T1 should be considered a sensitive marker for diseased myocardium, and not necessarily specific to the activity of the disease. This profile resembles the experience with EGE, which has also been found to remain increased even after clinical convalescence (65), as well as with LGE. The high overall negative predictive value of T1 mapping (NPV 92% (2)) makes it especially useful for ruling out myocardial inflammation.

Extracellular volume (ECV) mapping

ECV also detects an expanded extracellular space. In contrast to LGE imaging, ECV may also detect milder but global processes like diffuse edema and fibrosis, which may be very useful as an additional biomarker (40,71) for identifying changes not detected by LGE (72). More evidence is needed to demonstrate its incremental value beyond LGE in combination with the aforementioned CMR tissue characterization approaches, especially the native mapping techniques.

The diagnostic performance of various CMR criteria combinations

Figure 1 provides an overview of current evidence on the diagnostic accuracy of CMR in detecting acute myocarditis. The Original Lake Louise Criteria ("Any 2 out of 3") currently has the largest evidence base supporting its diagnostic performance in detecting acute myocardial inflammation. Removing EGE does not appear to substantially hamper the diagnostic performance of the Original Lake Louise Criteria, consistent with previous findings (58), and T2-weighted imaging combined with LGE ("2 out of 2") demonstrates a reasonable ability to detect acute myocarditis. Although other "2 out of 2" combinations, such as "T2W + EGE" or "LGE + EGE", are possible, their performance is reported by only one study of 45 cases.

In **Figure 1**, the diagnostic ability of CMR combination criteria for detecting myocarditis, as assessed using estimated area-under-curve (AUC*), indicate varied performance, even within a particular combination (e.g. T2W/EGE/LGE). This may be driven in part by the desire to optimise sensitivity over the specificity, which decreases the AUC*. Similar conclusions may be drawn from meta-analysis of currently available published data (**Online Appendix**). While various statistical approaches are possible (3), they are subject to the choice of methods and assumptions made about the underlying data distributions (73, 74). Most importantly, summary comparisons conceal the high degree of heterogeneity in published reports, as demonstrated in

F**igure 1** (see also supplemental material for formal measures of heterogeneity). Despite these limitations in performing summary statistics on currently available data, it appears clear that novel mapping techniques offer at least theoretical advantage over the Original Lake Louise Criteria.

The following proposed update of the Lake Louise Criteria represent a "2 out of 2" approach, requiring one positive T2-based criterion and one T1-based criterion. The combination of T2-mapping and LGE provides a very good accuracy, although this is based on only 2 published studies thus far (52,66). A gadolinium-free protocol, combining T2-based CMR with T1-mapping, is highly attractive and may be very useful in cases where the administration of contrast agents is not desirable, although further studies are warranted.

Combining T2-mapping and ECV may theoretically improve diagnostic confidence in cases where global myocardial edema predominates, LGE is negative and if the diagnostic quality of T2-weighted imaging is impaired by technical issues; further evidence is needed for this approach.

While the combination of T1-mapping with LGE achieved a high diagnostic performance in published studies, and some data suggest that the degree of T1 increase is different between edema from diffuse fibrosis, it remains unclear whether native T1 can differentiate acute inflammation from chronic injury or diffuse fibrosis.

Quantitative mapping is a nascent field, with emerging evidence of its clinical utility, especially in aiding the non-invasive diagnosis of myocarditis. More head-to-head studies comparing mapping to conventional CMR imaging techniques are needed to establish their true diagnostic performance relative to each other in the detection of myocarditis. Longitudinal and multi-center studies to establish the prognostic power of these promising imaging biomarkers

and how they may guide treatment, specifically in inflammatory myocardial diseases, would further add to the clinical value of mapping techniques.

Update to the Lake Louise Criteria

Based on established statistical methods (75), the diagnostic accuracy can be significantly improved by combining edema-sensitive CMR (T2-w images or T2-mapping) with at least one additional T1-based tissue characterization technique (**Table 3**).

Based on currently available clinical evidence, the consensus group recommends that, in patients with a significant clinical pre-test probability (12), a CMR scan provides strong evidence for acute myocardial inflammation, if at least one criterion in each of the following 2 categories is positive (**Central Illustration**):

T2-based marker for myocardial edema

Methods: T2-weighted imaging or T2-mapping

Rationale: Because edema is an essential component of acute or active inflammation, the presence of a specific marker for edema (either on T2-weighted images or T2-mapping) is considered mandatory. T2, as measured by T2-mapping, is a reliable marker for myocardial edema, and is recommended as an alternative to T2-weighted CMR images.

T1-based marker for associated myocardial injury

Methods: LGE, T1-mapping or ECV

Rationale: LGE detects acute myocyte necrosis, focal fibrosis and scarring, and to some extent, acute extracellular edema. Native T1 relaxation time is prolonged by intra- or extra-cellular edema, hyperemia and capillary leak, and in areas of myocyte necrosis and fibrosis in myocarditis. ECV may be expanded by extracellular edema, hyperemia/ capillary leak, and in areas of necrosis and fibrosis.

Reporting of CMR Results

The evaluation of CMR images for acute inflammation should follow standard recommendations (76) and ensure that artefacts and areas with inadequate image quality are excluded from the analysis. The evaluation should be performed qualitatively (regional function, regional edema, regional necrosis/scarring, pericardial effusion) and quantitatively (for signal intensity ratios and mapping). For the quantitative assessment, certified post-processing and evaluation software with the capability to accurately quantify signal intensities, areas, volumes and relaxation parameters should be used. The signal intensity in skeletal muscle for the calculation of the T2 SI ratio should be measured in the serratus anterior muscle if accessible (77). The CMR reader should remain mindful of the likely presence or absence of underlying non-inflammatory myocardial disease causing diffuse fibrosis or infiltration, which may have a confounding effect when interpreting the significance of T1 prolongation detected by myocardial mapping. Table 4 lists the evaluation and parameters to be reported.

Utility of CMR in Specific Clinical Scenarios

Table 5 provides an overview of CMR features in myocardial inflammation per disease acuity and etiology.

Clinical presentation suggesting acute onset myocardial inflammation

In patients presenting with symptoms indicating acute myocardial injury, it is critically important to rule out acute coronary syndrome. While CMR is a very useful tool for identifying acute coronary syndrome, any additional diagnostic procedure may delay urgently required revascularization, especially in patients with a significant pre-test likelihood of coronary artery disease. In patients with low atherosclerotic risk, such as young patients without risk factors, however, acute myocardial inflammation caused by infectious or auto-immune disease is much

more likely than an ischemic event, and, thus, CMR may be considered a first-line diagnostic tool. The protocol should include full coverage of the LV applying edema-sensitive techniques. This approach is helpful to detect small areas of regional edema.

While the Lake Louise Criteria are only suitable for patients with suspected active/acute inflammation, CMR has demonstrated its utility in identifying inflammation in various chronic inflammatory conditions, ranging from chronic myocarditis to sarcoidosis to human immunodeficiency virus (HIV) disease. LGE has been commonly used, as has T2-weighted imaging, but parametric mapping is beginning to show its merit, especially for identifying ongoing inflammation in chronic cases.

Clinical scenarios can be classified according to their symptoms:

Infarct-like acute myocarditis

Clinically severe myocarditis with ST elevation and increased troponin levels is a presentation found mostly in acute viral myocarditis of younger patients, especially men (78-80). Prognostic data on this pattern are still scarce, yet it may be associated with a worse outcome (79). The CMR findings are typically impressive, with widespread edema and patchy, often inferolateral, necrosis in LGE images (79, 80). Therefore, in this setting, the Lake Louise criteria have a very high sensitivity and, given the distinct regional distribution pattern of injury, high specificity. In select institutions, immediate access to CMR may obviate coronary angiography in young patients without atherosclerotic risk factors and a recent history consistent with acute myocarditis.

New Onset Heart Failure

Heart failure is caused by either systolic dysfunction or by impaired filling with increased intraventricular pressure. Therefore, a more extensive myocardial involvement would be

expected. In the absence of symptoms indicating acute inflammation, this scenario typically reflects a previous episode of severe inflammatory injury with subsequent extensive scarring. Acute giant-cell myocarditis is known for its often-fulminant course with overt, sudden-onset heart failure, but any severe inflammation could cause sufficient damage.

Arrythmia

Myocardial inflammation and scars can lead to various forms of arrhythmia, including AV block, supraventricular or ventricular premature complexes, and even fatal arrhythmias such as ventricular fibrillation. The diagnostic workup of patients with unexplained arrhythmia therefore should include myocardial tissue characterization. Myocardial scars can often be associated with the electrocardiographic localization of arrhythmic foci.

Specific aspects related to certain etiologies of acute myocardial inflammation

While inflammation per se is non-specific, its severity, regional distribution, involvement of anatomical structures, and impact on pathophysiology often affect its presentation in CMR images.

Viral Myocarditis

Viral infections frequently affect the heart. While mostly benign, viral myocarditis may be severe and present with acute heart failure or, typically in young men, with "infarct-like" symptoms and findings (ST elevation, positive seromarkers for myocardial necrosis). CMR is the only diagnostic modality that can non-invasively identify myocardial edema, with or without necrosis, providing a specific marker for acute inflammation, including its severity and localization. CMR, thus, plays an important role for diagnostic and therapeutic decision-making in patients with acute viral myocarditis. CMR however cannot differentiate acute viral infection from a secondary immune response. The most frequent pattern includes subepicardial layers of

edema and necrosis, with a predominant involvement of the lateral and inferolateral wall of the left ventricle.

CMR has also been proven useful for the identification of chronic viral myocarditis (63), although its utility is less well established than in acute myocarditis. LGE is an important finding and is seen in up to 70% of patients with biopsy-proven chronic inflammation in the setting of heart failure (81). The presence of pericardial effusion is nonspecific and not particularly helpful in the diagnosis of chronic myocarditis as it was seen in only 28 of 62 such patients (82). In the MyoRacer study, EMB was used as the gold standard for establishing the diagnosis of myocarditis (15). Sixty-eight patients with chronic symptoms and a mean EF of 27% were studied. Seventy-one percent of the chronic patients were diagnosed with myocarditis by EMB, with a collagen volume fraction of 14±9%. Of all conventional Lake Louise Criteria and novel mapping techniques, only T2 mapping was found to be sufficiently diagnostic in chronic myocarditis, with an area under the receiver operating characteristic curve of 0.77, higher than for the LLC I criteria (0.53) and native T1 (0.53). One study of patients with acute myocarditis and those in clinical convalescence also showed that, although significantly increased T1 values in the acute stage diminish in the convalescent stage, they remain elevated compared to normal (68). Another study of 24 patients with active myocarditis showed that all CMR markers of inflammation showed normalization by 5 weeks after presentation (48).

Acute giant-cell myocarditis

The diagnosis of acute giant-cell myocarditis is of particular importance, because immediate treatment with immunosuppressive agents may improve outcome of this typically fulminant disease (83). The CMR appearance of giant-cell myocarditis has not been systematically studied, but reports and personal experience from experts indicate various forms

of tissue pathology, including the presence of large areas of high signal intensity in various, sometimes atypically subendocardial layers of the myocardium (84-86), similar to severe forms of sarcoidosis (87). The value of CMR, thus, will be the confirmation of widespread yet non-ischemic necrosis in acute cases.

Eosinophilic myocarditis

Eosinophilic myocarditis can be caused by hypersensitivity, allergy, drug sensitivity, neoplasia, drugs, vasculitis, and hematologic disorders (37). Different from the more subepicardial or patchy intramyocardial distribution patterns of viral myocarditis, eosinophilic myocarditis tends to display diffuse subendocardial areas of high signal intensity in late gadolinium enhancement images (37).

Myocarditis in pediatric populations

In children, cardiomyopathy due to myocarditis may present with fulminant heart failure requiring hemodynamic support (88). In this setting, CMR may provide diagnostic and prognostic value (89). The use of CMR is increasing, with 28% of children hospitalized for myocarditis having a CMR in 2011 (90). As in adults, the presence of LGE correlates with a greater risk of assist device implantation, transplantation or death (91).

Autoimmune Myocarditis

Systemic autoimmune diseases and vasculitides are associated with myocardial inflammation. In a study of 39 patients with rheumatoid arthritis and 29 matched controls, focal LGE was noted in 46% of patients, and patients had larger areas of myocardial edema on T2-w imaging (10% vs 0% of LV myocardium in controls), higher native T1 and ECV(92). A similar study in 60 females with RA showed a prevalence of LGE of 55% as well as higher native T1 (93). In systemic sclerosis, a study of 19 patients showed focal LGE in 10 (53%) as well as

higher native T1 and ECV and areas of elevated T2 signal (94). Native T1 and ECV correlated with disease activity and abnormal systolic and diastolic strain. Another study of 40 patients with systemic sclerosis showed a lower incidence of LGE (17.5%), primarily in the basal and mid septum and RV insertion sites (95).

Systemic Lupus Erythematosus

In systemic lupus erythematosus (SLE), a study of 20 patients showed that T2 ratio and EGE ratio were increased, which correlated with disease activity (96). LGE was noted in 3 of 8 patients examined. A more recent study noted LGE in 9 of 13 SLE subjects (97). Another study of 33 SLE patients demonstrated increased native T1 and ECV compared to controls (98). In addition, diffuse coronary vessel wall contrast enhancement was noted in 89% of 27 patients studied (99). Thus, CMR tissue characterization, including the novel mapping techniques, can detect subclinical myocarditis as part of systemic auto-immune diseases.

Pheochromocytoma and Catecholamine-Associated Myocarditis

Pheochromocytoma is associated with catecholamine-associated myocardial inflammation, which is demonstrable using multiparametric CMR, including T1-mapping. A systematic CMR study characterized the cardiac phenotype in 60 patients with pheochromocytoma compared to healthy and hypertensive controls (100). This study showed that subclinical catecholamine-myocarditis was frequent in patients with pheochromocytoma, which can lead to focal or diffuse fibrosis, and residual impairment of systolic and diastolic strain parameters even after curative surgery. These effects surpass those of hypertensive heart disease alone, supporting a direct role of catecholamine toxicity that may produce subtle but long-lasting myocardial alterations.

A similar pathophysiology exists in stress-induced cardiomyopathy (Takotsubo), that has been found to exhibit the CMR features of myocardial inflammation, albeit typically without significant abnormalities in LGE images (101).

Cardiac Sarcoidosis

Several studies have demonstrated the utility of LGE to identify cardiac involvement in sarcoidosis. One study of 81 patients showed an incidence of 26% of LGE, much higher than the 12% of patients identified by the Japanese Ministry of Health criteria (102). In the largest cohort studied to date, 152 patients with extracardiac sarcoidosis underwent CMR, and the incidence of LGE was 19% (103). Similarly, the incidence of focal LGE in another study of 28 patients with systemic sarcoidosis was 21% (104). In this study, however, T2 values were paradoxically lower in these regions of LGE. A small study of 8 patients with sarcoidosis imaged serially showed that, in the 6 of 8 that received adequate immunosuppressive therapy, T2 values declined from 70.0±5.5 to 59.2±6.1ms, which were associated with improvement in clinical markers of disease (105). A more recent systematic study incorporated CMR cine, LGE and all novel mapping techniques, to assess for myocardial involvement in 61 patients with sarcoidosis (106). It was found that native T1 mapping was the best discriminator between patients and healthy controls. This study demonstrated that mapping offers incremental value in detecting subclinical myocardial involvement when LGE and LV systolic function were unrevealing.

Hyperthyroidism

In 50 patients with hyperthyroidism 1-3 months after euthyroidism with therapy, CMR findings consistent with myocarditis were noted in 15 (30%) (107). Eight of the 15 patients demonstrated LGE and, on the whole, they demonstrated elevated T2 and EGE ratios.

Myocarditis in this setting was thought to be autoimmune due to the presence of circulating anti-microsomal and anti-thyroglobulin antibodies.

Others

CMR techniques often demonstrate inflammation in other systemic infectious conditions. In Chagas disease, one study of 51 patients showed evidence of LGE in 69% of patients and the prevalence correlate with clinical severity of disease (108). A more recent study of 54 patients showed that 78% of patients had elevated T2 signal intensity which correlated with the presence of LGE, and 74% had evidence of higher EGE ratio (109). In a study of 28 asymptomatic patients with chronic HIV infection, LGE was seen in 82%, primarily subepicardial (110). In addition, native T1, EGE and T2 ratios were elevated compared to normal subjects. In a study with 103 HIV-treated individuals without known cardiac disease (111), CMR demonstrated higher rates of subclinical myocardial edema, fibrosis, frequent pericardial effusions, and changes in myocardial structure and function.

Peripartum cardiomyopathy may involve myocardial inflammation, but data are still emerging. Recently, Checkpoint Inhibitor-mediated Myocarditis has been identified as a clinical entity that may benefit from including CMR in its diagnostic workup (7).

Summary and Outlook

Despite the substantial heterogeneity and high risk of bias (mainly due to design issues) of most published reports to-date (3), current evidence supports the use of CMR as a non-invasive means to detect signs of acute myocardial inflammation. In a clinical workup of a patient with suspected active myocardial inflammation, CMR evidence is based on at least one T2-based criterion (global or regional increase of myocardial T2 relaxation time or an increased signal intensity in T2-weighted CMR images), in combination with at least one T1-based

criterion (increased myocardial T1, increased extracellular volume, or increased signal intensity in Late Gadolinium Enhancement images).

CMR should be used in clinical trials of novel treatment options for diseases with significant myocardial inflammation, as this may overcome limitations of previous trials that were not able to demonstrate a therapeutic benefit.

References

1. Friedrich MG, Sechtem U, Schulz-Menger J, et al. Cardiovascular magnetic resonance in myocarditis: A JACC White Paper. J Am Coll Cardiol. 2009:53;1475–1487.

2. Lagan J, Schmitt M, Miller CA. Clinical applications of multi-parametric CMR in myocarditis and systemic inflammatory diseases. Int J Cardiovasc Imaging 2017;93:1–20.

3. Kotanidis CP, Bazmpani M-A, Haidich A-B, Karvounis C, Antoniades C, Karamitsos TD. Diagnostic Accuracy of Cardiovascular Magnetic Resonance in Acute Myocarditis: A Systematic Review and Meta-Analysis. JACC: Cardiovasc Img 2018.

4. Laissy J-P, Hyafil F, Feldman LJ, et al. Differentiating acute myocardial infarction from myocarditis: diagnostic value of early- and delayed-perfusion cardiac MR imaging. Radiology 2005;237:75–82.

5. Ferreira VM, Piechnik SK, Dall'armellina E, et al. T1 Mapping for the Diagnosis of Acute Myocarditis Using CMR: Comparison to T2-Weighted and Late Gadolinium Enhanced Imaging. JCMG 2013;6:1048–1058.

6. Kindermann I, Barth C, Mahfoud F, et al. Update on myocarditis. J Am Coll Cardiol 2012;59:779–792.

7. Mahmood SS, Fradley MG, Cohen JV, et al. Myocarditis in Patients Treated With Immune Checkpoint Inhibitors. J Am Coll Cardiol 2018;71:1755–1764.

8. Fung G, Luo H, Qiu Y, Yang D, McManus B. Myocarditis. Circ Res 2016;118:496–514.

9. Heymans S, Eriksson U, Lehtonen J, Cooper LT. The Quest for New Approaches in Myocarditis and Inflammatory Cardiomyopathy. J Am Coll Cardiol 2016;68:2348–2364.

10. Maron BJ, Udelson JE, Bonow RO, et al. Eligibility and Disqualification Recommendations for Competitive Athletes With Cardiovascular Abnormalities: Task Force 3: Hypertrophic

Cardiomyopathy, Arrhythmogenic Right Ventricular Cardiomyopathy and Other Cardiomyopathies, and Myocarditis: A Scientific Statement From the American Heart Association and American College of Cardiology. J Am Coll Cardiol 2015;66:2362–2371.

11. Cooper LT Jr. Myocarditis. N Engl J Med 2009;360:1526–1538.

12. Caforio ALP, Pankuweit S, Arbustini E, et al. Current state of knowledge on aetiology, diagnosis, management, and therapy of myocarditis: a position statement of the European Society of Cardiology Working Group on Myocardial and Pericardial Diseases. In: Vol 34. 2013:2636–48– 2648a–2648d.

13. Bozkurt B, Colvin M, Cook J, et al. Current Diagnostic and Treatment Strategies for Specific Dilated Cardiomyopathies: A Scientific Statement From the American Heart Association. Circulation 2016;134:e579–e646.

14. Ponikowski P, Voors AA, Anker SD, et al. 2016 ESC Guidelines for the diagnosis and treatment of acute and chronic heart failure: The Task Force for the diagnosis and treatment of acute and chronic heart failure of the European Society of Cardiology (ESC)Developed with the special contribution of the Heart Failure Association (HFA) of the ESC. Eur Heart J 2016;37:2129–2200.

15. Lurz P, Luecke C, Eitel I, et al. Comprehensive Cardiac Magnetic Resonance Imaging in Patients With Suspected Myocarditis. J Am Coll Cardiol 2016;67:1800–1811.

16. Schumm J, Greulich S, Wagner A, et al. Cardiovascular magnetic resonance risk stratification in patients with clinically suspected myocarditis. Journal of Cardiovascular Magnetic Resonance 2014;16:1–12.

17. Vermes E, Childs H, Faris P, Friedrich MG. Predictive value of CMR criteria for LV functional improvement in patients with acute myocarditis. European Heart Journal

Cardiovascular Imaging 2014;15:1140–1144.

18. Boehmer JP, Starling RC, Cooper LT, et al. Left ventricular assist device support and myocardial recovery in recent onset cardiomyopathy. J Card Fail 2012;18:755–761.

19. Jeserich M, Brunner E, Kandolf R, et al. Diagnosis of viral myocarditis by cardiac magnetic resonance and viral genome detection in peripheral blood. Int J Cardiovasc Imaging 2012.

20. Lurz P, Eitel I, Adam J, et al. Diagnostic Performance of CMR Imaging Compared With EMB in Patients With Suspected Myocarditis. JACC: Cardiovasc Img 2012;5:513–524.

21. Ukena C, Mahfoud F, Kindermann I, Kandolf R, Kindermann M, Böhm M. Prognostic electrocardiographic parameters in patients with suspected myocarditis. European Journal of Heart Failure 2011;13:398–405.

22. Ukena C, Kindermann M, Mahfoud F, et al. Diagnostic and prognostic validity of different biomarkers in patients with suspected myocarditis. Clin Res Cardiol 2014;103:743–751.

23. Mahfoud F, Gärtner B, Kindermann M, et al. Virus serology in patients with suspected myocarditis: utility or futility? Eur Heart J 2011;32:897–903.

24. Florian A, Schäufele T, Ludwig A, et al. Diagnostic value of CMR in young patients with clinically suspected acute myocarditis is determined by cardiac enzymes. Clin Res Cardiol 2015;104:154–163.

25. Yilmaz A, Klingel K, Kandolf R, Sechtem U. Imaging in inflammatory heart disease: from the past to current clinical practice. Hellenic J Cardiol 2009;50:449–460.

26. Nensa F, Kloth J, Tezgah E, et al. Feasibility of FDG-PET in myocarditis: Comparison to CMR using integrated PET/MRI. J Nucl Cardiol 2016:1–10.

27. Yilmaz A, Kindermann I, Kindermann M, et al. Comparative evaluation of left and right ventricular endomyocardial biopsy: differences in complication rate and diagnostic performance.

Circulation 2010;122:900–909.

28. Cooper LT, Baughman KL, Feldman AM, et al. The role of endomyocardial biopsy in the management of cardiovascular disease: A Scientific Statement from the American Heart Association, the American College of Cardiology, and the European Society of Cardiology Endorsed by the Heart Failure Society of America and the Heart Failure Association of the European Society of Cardiology. Eur Heart J 2007;28:3076–3093.

29. Ardehali H, Qasim A, Cappola T, et al. Endomyocardial biopsy plays a role in diagnosing patients with unexplained cardiomyopathy. American Heart journal 2004;147:919–923.

30. Kindermann I, Kindermann M, Kandolf R, et al. Predictors of Outcome in Patients With Suspected Myocarditis. Circulation 2008;118:639–648.

31. Baccouche H, Mahrholdt H, Meinhardt G, et al. Diagnostic synergy of non-invasive cardiovascular magnetic resonance and invasive endomyocardial biopsy in troponin-positive patients without coronary artery disease. Eur Heart J 2009;30:2869–2879.

32. Fernández-Jiménez R, Sánchez-González J, Aguero J, et al. Fast T2 gradient-spin-echo (T2-GraSE) mapping for myocardial edema quantification: first in vivo validation in a porcine model of ischemia/reperfusion. J Cardiovasc Magn Reson 2015;17:92.

33. Ferreira VM, Piechnik SK, Dall'armellina E, et al. Non-contrast T1-mapping detects acute myocardial edema with high diagnostic accuracy: a comparison to T2-weighted cardiovascular magnetic resonance. J Cardiovasc Magn Reson 2012;14:42.

34. Iles LM, Ellims AH, Llewellyn H, et al. Histological validation of cardiac magnetic resonance analysis of regional and diffuse interstitial myocardial fibrosis. European Heart J Cardiovascular Imaging 2015;16:14–22.

35. Verbrugge FH, Bertrand PB, Willems E, et al. Global myocardial oedema in advanced

decompensated heart failure. European Heart Journal Cardiovascular Imaging 2017;18:787–794.

36. Zarka S, Bouleti C, Arangalage D, et al. Usefulness of Subepicardial Hyperemia on Contrast-Enhanced First-Pass Magnetic Resonance Perfusion Imaging for Diagnosis of Acute Myocarditis. Am J Cardiol 2016;118:440–445.

37. Kuchynka P, Palecek T, Masek M, et al. Current Diagnostic and Therapeutic Aspects of Eosinophilic Myocarditis. Biomed Research International 2016;2016:2829583–6.

38. Bogaert J, Francone M. Cardiovascular magnetic resonance in pericardial diseases. J Cardiovasc Magn Reson 2009;11:14.

39. Thavendiranathan P, Walls M, Giri S, et al. Improved detection of myocardial involvement in acute inflammatory cardiomyopathies using T2 mapping. Circ Cardiovasc Imaging 2012;5:102–110.

40. Radunski UK, Lund GK, Stehning C, et al. CMR in patients with severe myocarditis: diagnostic value of quantitative tissue markers including extracellular volume imaging. JACC: Cardiovasc Img 2014;7:667–675.

41. Kellman P, Wilson JR, Xue H, Ugander M, Arai AE. Extracellular volume fraction mapping in the myocardium, part 1: evaluation of an automated method. J Cardiovascular Magnetic Resonance 2012;14:1–1.

42. Ferreira VM, Piechnik SK, Dall'armellina E, et al. Native T1-mapping detects the location, extent and patterns of acute myocarditis without the need for gadolinium contrast agents. J Cardiovasc Magn Reson 2014;16:36.

43. Baeßler B, Schaarschmidt F, Stehning C, Schnackenburg B, Maintz D, Bunck AC. A systematic evaluation of three different cardiac T2-mapping sequences at 1.5 and 3T in healthy volunteers. Eur J Radiol 2015;84:2161–2170.

44. Moon JC, Messroghli DR, Kellman P, et al. Myocardial T1 mapping and extracellular volume quantification: a Society for Cardiovascular Magnetic Resonance (SCMR) and CMR Working Group of the European Society of Cardiology consensus statement. J Cardiovasc Magn Reson 2013;15:92.

45. Aletras AH, Kellman P, Derbyshire JA, Arai AE. ACUT2E TSE-SSFP: A hybrid method for T2-weighted imaging of edema in the heart. Magn Reson Med 2008;59:229–235.

46. van Heeswijk RB, Feliciano H, Bongard C, et al. Free-breathing 3 T magnetic resonance T2-mapping of the heart. JACC: Cardiovasc Img 2012;5:1231–1239.

47. Messroghli DR, Moon JC, Ferreira VM, et al. Clinical recommendations for cardiovascular magnetic resonance mapping of T1, T2, T2* and extracellular volume: A consensus statement by the Society for Cardiovascular Magnetic Resonance (SCMR) endorsed by the European Association for Cardiovascular Imaging (EACVI). J Cardiovasc Magn Reson 2017;19:42–24.

48. Luetkens JA, Homsi R, Dabir D, et al. Comprehensive Cardiac Magnetic Resonance for Short-Term Follow-Up in Acute Myocarditis. J Am Heart Association 2016;5:e003603.

49. Robson MD, Piechnik SK, Tunnicliffe EM, Neubauer S. T1 measurements in the human myocardium: the effects of magnetization transfer on the SASHA and MOLLI sequences. Magnetic Resonance Medicine 2013;70:664–670.

50. Simonetti OP, Finn JP, White RD, Laub G, Henry DA. "Black blood" T2-weighted inversion-recovery MR imaging of the heart. Radiology 1996;199:49–57.

51. O h-Ici D, Ridgway JP, Kuehne T, et al. Cardiovascular magnetic resonance of myocardial edema using a short inversion time inversion recovery (STIR) black-blood technique: Diagnostic accuracy of visual and semi-quantitative assessment. J Cardiovasc Magn Reson 2012;14:22.

52. Knobelsdorff-Brenkenhoff von F, Schüler J, Doganguzel S, et al. Detection and Monitoring

of Acute Myocarditis Applying Quantitative Cardiovascular Magnetic Resonance. Circ Cardiovasc Imaging 2017;10:e005242.

53. Kumar A, Beohar N, Arumana JM, et al. CMR Imaging of Edema in Myocardial Infarction Using Cine Balanced Steady-State Free Precession. JACC: Cardiovasc Img 2011;4:1265–1273.

54. De Lazzari M, Zorzi A, Baritussio A, et al. Relationship between T-wave inversion and transmural myocardial edema as evidenced by cardiac magnetic resonance in patients with clinically suspected acute myocarditis: clinical and prognostic implications. J Electrocardiol 2016;49:587–595.

55. Nordlund D, Klug G, Heiberg E, et al. Multi-vendor, multicentre comparison of contrast-enhanced SSFP and T2-STIR CMR for determining myocardium at risk in ST-elevation myocardial infarction. European Heart Journal Cardiovascular Imaging 2016;17:744–753.

56. Kellman P, Aletras AH, Mancini C, McVeigh ER, Arai AE. T2-prepared SSFP improves diagnostic confidence in edema imaging in acute myocardial infarction compared to turbo spin echo. Magn Reson Med 2007;57:891–897.

57. Laissy J-P, Messin B, Varenne O, et al. MRI of acute myocarditis: a comprehensive approach based on various imaging sequences. Chest 2002;122:1638–1648.

58. Chu GCW, Flewitt JA, Mikami Y, Vermes E, Friedrich MG. Assessment of acute myocarditis by cardiovascular MR: diagnostic performance of shortened protocols. Int J Cardiovasc Imaging 2013;29:1077–1083.

59. Ammirati E, Moroni F, Sormani P, et al. Quantitative changes in late gadolinium enhancement at cardiac magnetic resonance in the early phase of acute myocarditis. Int. J. Cardiol. 2017;231:216–221.

60. Schwab J, Rogg HJ, Pauschinger M, et al. Functional and Morphological Parameters with

Tissue Characterization of Cardiovascular Magnetic Imaging in Clinically Verified "Infarct-like Myocarditis." Rofo Fortschr Geb Rontgenstr Neuen Bildgeb Verfahr 2015;188:365–373.

61. Verhaert D, Thavendiranathan P, Giri S, et al. Direct T2 Quantification of Myocardial Edema in Acute Ischemic Injury. JACC: Cardiovasc Img 2011;4:269–278.

62. Spieker M, Haberkorn S, Gastl M, et al. Abnormal T2 mapping cardiovascular magnetic resonance correlates with adverse clinical outcome in patients with suspected acute myocarditis. J Cardiovasc Magn Reson 2017;19:38.

63. Gutberlet M, Spors B, Thoma T, et al. Suspected Chronic Myocarditis at Cardiac MR: Diagnostic Accuracy and Association with Immunohistologically Detected Inflammation and Viral Persistence. Radiology 2008;246:401–409.

64. Francone M, Chimenti C, Galea N, et al. CMR Sensitivity Varies With Clinical Presentation and Extent of Cell Necrosis in Biopsy-Proven Acute Myocarditis. JACC: Cardiovasc Img 2014.

65. Bohnen S, Radunski UK, Lund GK, et al. T1 mapping cardiovascular magnetic resonance imaging to detect myocarditis-Impact of slice orientation on the diagnostic performance. Eur J Radiol 2017;86:6–12.

66. Luetkens JA, Homsi R, Sprinkart AM, et al. Incremental value of quantitative CMR including parametric mapping for the diagnosis of acute myocarditis. European Heart Journal Cardiovascular Imaging 2016;17:154–161.

67. Luetkens JA, Doerner J, Thomas DK, et al. Acute myocarditis: multiparametric cardiac MR imaging. Radiology 2014;273:383–392.

68. Hinojar R, Foote L, Arroyo Ucar E, et al. Native T1 in Discrimination of Acute and Convalescent Stages in Patients With Clinical Diagnosis of Myocarditis: A Proposed Diagnostic Algorithm Using CMR. JACC: Cardiovasc Img 2015;8:37–46.

69. Kali A, Choi E-Y, Sharif B, et al. Native T1 Mapping by 3-T CMR Imaging for Characterization of Chronic Myocardial Infarctions. JACC: Cardiovasc Img 2015;8:1019–1030.

70. Liu D. CMR native T1 mapping differentiates reversible vs. irreversible myocardial damage in STEMI. 2016:1–28.

71. Nadjiri J, Nieberler H, Hendrich E, et al. Performance of native and contrast-enhanced T1 mapping to detect myocardial damage in patients with suspected myocarditis : a head-to-head comparison of different cardiovascular magnetic resonance techniques. Int J Cardiovasc Imaging 2016:1–9.

72. Radunski UK, Lund GK, Säring D, et al. T1 and T2 mapping cardiovascular magnetic resonance imaging techniques reveal unapparent myocardial injury in patients with myocarditis. Clin Res Cardiol 2016:1–8.

73. Bandos AI, Guo B, Gur D. Estimating the Area Under ROC Curve When the Fitted Binormal Curves Demonstrate Improper Shape. Acad Radiol 2017;24:209–219.

74. Marzban C. The ROC Curve and the Area under It as Performance Measures. Weather and Forecasting 2004;19:1106–1114. Available at: https://doi.org/10.1175/825.1.

75. Weinstein S, Obuchowski NA, Lieber ML. Clinical evaluation of diagnostic tests. AJR Am J Roentgenol 2005;184:14–19.

76. Schulz-Menger J, Bluemke DA, Bremerich J, et al. Standardized image interpretation and post processing in cardiovascular magnetic resonance: Society for Cardiovascular Magnetic Resonance (SCMR) Board of Trustees Task Force on Standardized Post Processing. J Cardiovasc Magn Reson 2013;15:35.

77. Carbone I, Childs H, Aljizeeri A, Merchant N, Friedrich MG. Importance of Reference

Muscle Selection in Quantitative Signal Intensity Analysis of T2-Weighted Images of Myocardial Edema Using a T2 Ratio Method. Biomed Research International 2015;2015:1–10.

78. Cocker MS, Abdel-Aty H, Strohm O, Friedrich MG. Age and gender effects on the extent of myocardial involvement in acute myocarditis: a cardiovascular magnetic resonance study. Heart 2009;95:1925–1930.

79. Chopra H, Arangalage D, Bouleti C, et al. Prognostic value of the infarct- and non-infarct like patterns and cardiovascular magnetic resonance parameters on long-term outcome of patients after acute myocarditis. Int. J. Cardiol. 2016;212:63–69.

80. Faletti R, Gatti M, Baralis I, et al. Clinical and magnetic resonance evolution of "infarct-like" myocarditis. Radiol Med 2017;122:273–279.

81. De Cobelli F, Pieroni M, Esposito A, et al. Delayed Gadolinium-Enhanced Cardiac Magnetic Resonance in Patients With Chronic Myocarditis Presenting With Heart Failure or Recurrent Arrhythmias. J Am Coll Cardiol 2006;47:1649–1654.

82. Lurz P, Eitel I, Klieme B, et al. The potential additional diagnostic value of assessing for pericardial effusion on cardiac magnetic resonance imaging in patients with suspected myocarditis. European Heart Journal Cardiovascular Imaging 2014;15:643–650.

83. Cooper LT, ElAmm C. Giant cell myocarditis. Diagnosis and treatment. Herz 2012;37:632–636.

84. Shonk JR, Vogel-Claussen J, Halushka MK, Lima JAC, Bluemke DA. Giant cell myocarditis depicted by cardiac magnetic resonance imaging. Journal of computer assisted tomography 2005;29:742–744.

85. Azarine A, Guillemain R, Bruneval P. Different focal delayed gadolinium-enhancement patterns using cardiac magnetic resonance in a case of diffuse giant cell myocarditis. Eur Heart J

2009;30:1485.

86. Sujino Y, Kimura F, Tanno J, et al. Cardiac magnetic resonance imaging in giant cell myocarditis: intriguing associations with clinical and pathological features. Circulation 2014;129:e467–9.

87. Bogabathina H, Olson P, Rathi VK, Biederman RWW. Cardiac sarcoidosis or giant cell myocarditis? On treatment improvement of fulminant myocarditis as demonstrated by cardiovascular magnetic resonance imaging. Case Rep Cardiol 2012;2012:647041–5.

88. Ghelani SJ, Spaeder MC, Pastor W, Spurney CF, Klugman D. Demographics, trends, and outcomes in pediatric acute myocarditis in the United States, 2006 to 2011. Circ Cardiovasc Qual Outcomes 2012;5:622–627.

89. Banka P, Robinson JD, Uppu SC, et al. Cardiovascular magnetic resonance techniques and findings in children with myocarditis: a multicenter retrospective study. J Cardiovasc Magn Reson 2015;17:96.

90. Canter CE, Simpson KE. Diagnosis and Treatment of Myocarditis in Children in the Current Era. Circulation 2014;129:115–128.

91. Sachdeva S, Song X, Dham N, Heath DM, DeBiasi RL. Analysis of clinical parameters and cardiac magnetic resonance imaging as predictors of outcome in pediatric myocarditis. Am J Cardiol 2015;115:499–504.

92. Ntusi NAB, Piechnik SK, Francis JM, et al. Diffuse Myocardial Fibrosis and Inflammation in Rheumatoid Arthritis: Insights From CMR T1 Mapping. JACC: Cardiovasc Img 2015;8:526–536.

93. Holmström M, Koivuniemi R, Korpi K, et al. Cardiac magnetic resonance imaging reveals frequent myocardial involvement and dysfunction in active rheumatoid arthritis. Clin. Exp.

Rheumatol. 2016;34:416–423.

94. Ntusi NAB, Piechnik SK, Francis JM, et al. Subclinical myocardial inflammation and diffuse fibrosis are common in systemic sclerosis--a clinical study using myocardial T1-mapping and extracellular volume quantification. J Cardiovasc Magn Reson 2014;16:21.

95. Sano M, Satoh H, Suwa K, et al. Characteristics and clinical relevance of late gadolinium enhancement in cardiac magnetic resonance in patients with systemic sclerosis. Heart Vessels 2015;30:779–788.

96. Abdel-Aty H, Siegle N, Natusch A, et al. Myocardial tissue characterization in systemic lupus erythematosus: value of a comprehensive cardiovascular magnetic resonance approach. Lupus 2008;17:561–567.

97. Thomas G, Cohen Aubart F, Chiche L, et al. Lupus Myocarditis: Initial Presentation and Longterm Outcomes in a Multicentric Series of 29 Patients. J. Rheumatol. 2017;44:24–32.

98. Puntmann VO, Puntmann VO, D'Cruz D, et al. Native myocardial T1 mapping by cardiovascular magnetic resonance imaging in subclinical cardiomyopathy in patients with systemic lupus erythematosus. Circ Cardiovasc Imaging 2013;6:295–301.

99. Varma N, Hinojar R, D'Cruz D, et al. Coronary vessel wall contrast enhancement imaging as a potential direct marker of coronary involvement: integration of findings from CAD and SLE patients. JACC: Cardiovasc Img 2014;7:762–770.

100. Ferreira VM, Marcelino M, Piechnik SK, et al. Pheochromocytoma Is Characterized by Catecholamine-Mediated Myocarditis, Focal and Diffuse Myocardial Fibrosis, and Myocardial Dysfunction. J Am Coll Cardiol 2016;67:2364–2374.

101. Eitel I, Knobelsdorff-Brenkenhoff von F, Bernhardt P, et al. Clinical characteristics and cardiovascular magnetic resonance findings in stress (takotsubo) cardiomyopathy.

2011;306:277–286.

102. Patel MR, Cawley PJ, Heitner JF, et al. Detection of Myocardial Damage in Patients With Sarcoidosis. Circulation 2009;120:1969–1977.

103. Patel AR, Klein MR, Chandra S, et al. Myocardial damage in patients with sarcoidosis and preserved left ventricular systolic function: an observational study. European Journal of Heart Failure 2011;13:1231–1237.

104. Yang Y, Safka K, Graham JJ, et al. Correlation of late gadolinium enhancement MRI and quantitative T2 measurement in cardiac sarcoidosis. J Magn Reson Imaging 2014;39:609–616.

105. Crouser ED, Ruden E, Julian MW, Raman SV. Resolution of abnormal cardiac MRI T2 signal following immune suppression for cardiac sarcoidosis. J. Investig. Med. 2016;64:1148–1150.

106. Greulich S, Deluigi CC, Gloekler S, et al. CMR Imaging Predicts Death and Other Adverse Events in Suspected Cardiac Sarcoidosis. JCMG 2013;6:501–511.

107. Mavrogeni S, Markussis V, Bratis K, et al. Hyperthyroidism induced autoimmune myocarditis. Evaluation by cardiovascular magnetic resonance and endomyocardial biopsy. Int. J. Cardiol. 2012;158:166–168.

108. Rochitte CE, Oliveira PF, Andrade JM, et al. Myocardial delayed enhancement by magnetic resonance imaging in patients with Chagas' disease: a marker of disease severity. J Am Coll Cardiol 2005;46:1553–1558.

109. Torreão JA, Ianni BM, Mady C, et al. Myocardial tissue characterization in Chagas' heart disease by cardiovascular magnetic resonance. J Cardiovasc Magn Reson 2015;17:97.

110. Luetkens JA, Doerner J, Schwarze-Zander C, et al. Cardiac Magnetic Resonance Reveals Signs of Subclinical Myocardial Inflammation in Asymptomatic HIV-Infected Patients. Circ

Cardiovasc Imaging 2016;9:e004091.

111. Ntusi N, O'Dwyer E, Dorrell L, et al. HIV-1–Related Cardiovascular Disease Is Associated With Chronic Inflammation, Frequent Pericardial Effusions, and Probable Myocardial EdemaCLINICAL PERSPECTIVE. Circ Cardiovasc Imaging 2016;9:e004430–9.

112. Abdel-Aty H, Boyé P, Zagrosek A, et al. Diagnostic performance of cardiovascular magnetic resonance in patients with suspected acute myocarditis: comparison of different approaches. J Am Coll Cardiol 2005;45:1815–1822.

113. Knobelsdorff von F, Prothmann M, Dieringer MA, et al. Differentiation of acute and chronic myocardial infarction using T2-weighted imaging, late enhancement and T1 and T2 mapping - a pilot study at 3T. J Cardiovasc Magn Reson 2014;16:P222.

Figure Legends

Central Illustration. Overview of the updated Lake Louise Criteria. LGE: Late Gadolinium Enhancement; ECV: Extracellular Volume

Figure 1. Overview of the current evidence comparing the diagnostic performance of various CMR criteria combinations in detecting acute myocarditis. The Original Lake Louise Criteria I (left-most column; "Any 2 out of 3") is supported by the largest but heterogenous body of evidence. The evidence on other CMR criteria combinations is also heterogenous and much sparser. Nevertheless, the data suggest that novel mapping techniques may offer at least theoretical advantage over the Original Lake Louise Criteria, pending further validation. AUC*: estimated area-under-the-curve, calculated as the average of the sensitivity and specificity reported for each combination in published studies. The bubbles tend to rise towards higher values of AUC* for combinations that include mapping for at least one criterion. The radius of each bubble is proportional to the square-root of the study sample size. † Evidence base is expressed as "number of published studies" x "total number of cases from those studies". Data for Original Lake Louise Criteria from (15, 20, 40, 58, 60, 66, 67, 112), for T2 + EGE and EGE + LGE from (58), for T2W + LGE from (42, 52, 58), for T2 map + LGE from (52, 66) and for T1 map + LGE from (42, 52, 66, 67, 110), for T2-weighted imaging and T1 map from (42, 67), and for T1 map + T2 map from (113).

Table 1. Diagnostic tests and potential findings in patients with acute myocarditis (adapted from Caforio et al. (12))

(a) ECG/Holter/stress test

- AV-Block I-III°, bundle brunch block, sinus arrest
- extrasystoles
- supraventricular tachycardia, atrial fibrillation
- ventricular tachycardia, ventricular fibrillation, asystole
- ST and T-wave changes (ST elevation, T wave inversion)
- intraventricular conduction delay
- new Q-waves
- low voltage

(b) Seromarkers for myocardial necrosis

- Troponin elevation
- Creatine kinase elevation

(c) Cardiac imaging

- *Echocardiography/angiography*
    - regional or global systolic or diastolic dysfunction, with or without LV dilatation,
    - increased wall thickness
    - pericardial effusion
    - intracavitary thrombi
- *CMR*
    - Edema
    - Hyperemia/capillary leak (early gadolinium enhancement)
    - Irreversible injury (necrosis, scar; late gadolinium enhancement)
    - regional or global systolic or diastolic dysfunction, with or without LV dilatation,
    - increased wall thickness
    - pericardial effusion
    - intracavitary thrombi

Clinically suspected myocarditis if ≥1 clinical presentation and ≥1 diagnostic criteria from different categories, in the absence of: (1) angiographically detectable coronary artery disease (coronary stenosis ≥ 50%); (2) known pre-existing cardiovascular disease or extra-cardiac causes that could explain the syndrome (e.g. valve disease, congenital heart disease,

hyperthyroidism, etc.). Suspicion is higher with higher number of fulfilled criteria. If the patient is asymptomatic, ≥2 diagnostic criteria should be met.

Table 2. Descriptive statistics of currently available evidence comparing the diagnostic performance of CMR markers for the detection of acute myocarditis. (see also Figure 1 and Supplemental Material).

CMR Criteria	Median estimated area-under-the-curve AUC* (total range)	Number of published studies (n)	Total number of cases (n)
Individual			
T2-weighted (T2W) imaging	73 (58-100)	13	981
Early Gadolinium Enhancement	73 (62-93)	10	711
Late Gadolinium Enhancement	83 (53-96)	14	1073
T1-mapping	89 (71-99)	9	682
T2-mapping	80 (73-86)	6	449
Extracellular Volume	74 (59-82)	7	555
Combinations			
Original Lake Louise Criteria	84 (57-90)	8	630
T2W + LGE	76 (71-89)	3	191
T2W + EGE	75	1	45
EGE + LGE	70	1	45
T2-mapping + LGE	90 (83-97)	2	120
T2-mapping + T1-mapping	86	1	36
T2W + T1-mapping	84 (73-95)	2	176
T1-mapping + LGE	96 (82-97)	5	350

AUC* is the “estimated area-under-the-curve”, calculated as the average of the sensitivity and specificity reported for each combination in published studies; this allowed direct comparison of various combinations even for studies which did not provide the actual AUC. T2W =T2-weighted imaging; LGE = Late gadolinium enhancement; EGE = Early gadolinium enhancement; ECV: Extracellular Volume;

Table 3. Updated recommendations of CMR criteria of myocardial inflammation.

	Original Lake Louise Criteria I (Any 2 out of 3)	Updated Lake Louise Criteria II (2 out of 2)	Diagnostic Targets
	T2-weighted imaging	**T2-based imaging**	Myocardial edema
Main Criteria	Regional† high T2 SI *or* Global T2 SI ratio ≥2.0†† in T2-w CMR images	Regional† high T2 SI *or* Global T2 SI ratio ≥2.0†† in T2-w CMR images *or* Regional or global increase of myocardial T2 relaxation time††	
	Early Gadolinium Enhancement	**T1-based imaging**	↑ T1 – edema (intra or extra-cellular), hyperemia/ capillary leak, necrosis, fibrosis EGE – hyperemia, capillary leak LGE – necrosis, fibrosis, (extracellular acute edema) ↑ ECV – edema (extracellular), hyperemia/ capillary leak, necrosis, fibrosis
	SI ratio myocardium/skeletal muscle (EGE ratio) of ≥4.0†† in EGE images	Regional or global increase of native myocardial T1 relaxation time or ECV††§ *or* Areas with high SI in a non-ischemic distribution pattern in LGE images	
	Late Gadolinium Enhancement		
	Areas with high SI in a non-ischemic distribution pattern in LGE images		
Supportive Criteria	Pericardial effusion in cine CMR images	Pericardial effusion in cine CMR images *or* High signal intensity of the pericardium in LGE images *or* T1 mapping or T2 mapping	Pericardial inflammation
	Systolic LV wall motion abnormality in cine CMR images	Systolic LV wall motion abnormality in cine CMR images	LV dysfunction

†: "Regional" refers to an area of at least 10 contiguous pixels.
††: Published or local normal values, LV coverage and proper analysis tools must be acknowledged.
§: T1-mapping is highly sensitive to detecting both acute and chronic forms of increased free water content within the myocardium, and thus, the consensus group recommends treating it as an alternative criterion to EGE. If paired with LGE to diagnose myocarditis, the areas of T1 abnormality should be beyond that detected by LGE imaging.

Table 4. Evaluation of CMR images and parameters for reporting acute myocardial inflammation

CMR Parameters for reporting acute myocardial inflammation	
Ventricular function	• Presence/location of global or regional systolic dysfunction • Left ventricular end-diastolic volume (LVEDV) • Left ventricular end-systolic volume (LVESV) • Ejection fraction (EF) • Stroke volume (SV) and stroke volume index (SVI) • Cardiac index (CI)
Edema*	• Presence, extent and localization of visually apparent edema • T2 SI ratio or native T2
Hyperemia and capillary leakage	• Native T1 or ECV
Necrosis and fibrosis	• Presence, extent and localization of visually apparent necrosis or scar on LGE imaging • Native T1 or ECV
Pericardium	• Presence, extent and localization of effusion • Signal increase in LGE, T2- or T1-mapping • Pericardial thickness if >3mm • Hemodynamic relevance if applicable: evidence of constriction

*Native T1 and ECV are also sensitive to, although not specific for, myocardial inflammation and edema, as these parameters also reflect chronic changes, such as focal and diffuse myocardial fibrosis.

Table 5. CMR features in myocardial inflammation according to disease acuity and etiology

Presentation	Diseases	Pathology	Typical CMR findings	Disease-specific aspects
Acute (active)	Viral myocarditis Auto-immune Allergic Giant-cell myocarditis Other	edema hyperemia ±necrosis	T2 ↑ T1 ↑ LGE (-) or (+)	Intramural or subepicardial distribution; important to differentiate from ischemic injury
Chronic	Viral myocarditis Auto-immune Sarcoidosis Hyperthyroidism Other	±edema ±hyperemia ±necrosis ±regional fibrosis (scar) ±diffuse fibrosis	T2 (-) or ↑ T1 (-) or ↑ LGE (-) or (+)	ECV may provide incremental information
Healed	All	±regional fibrosis (scar) ±diffuse fibrosis	T2 (-) T1 (-) or ↑ LGE (-) or (+)	ECV may provide incremental information

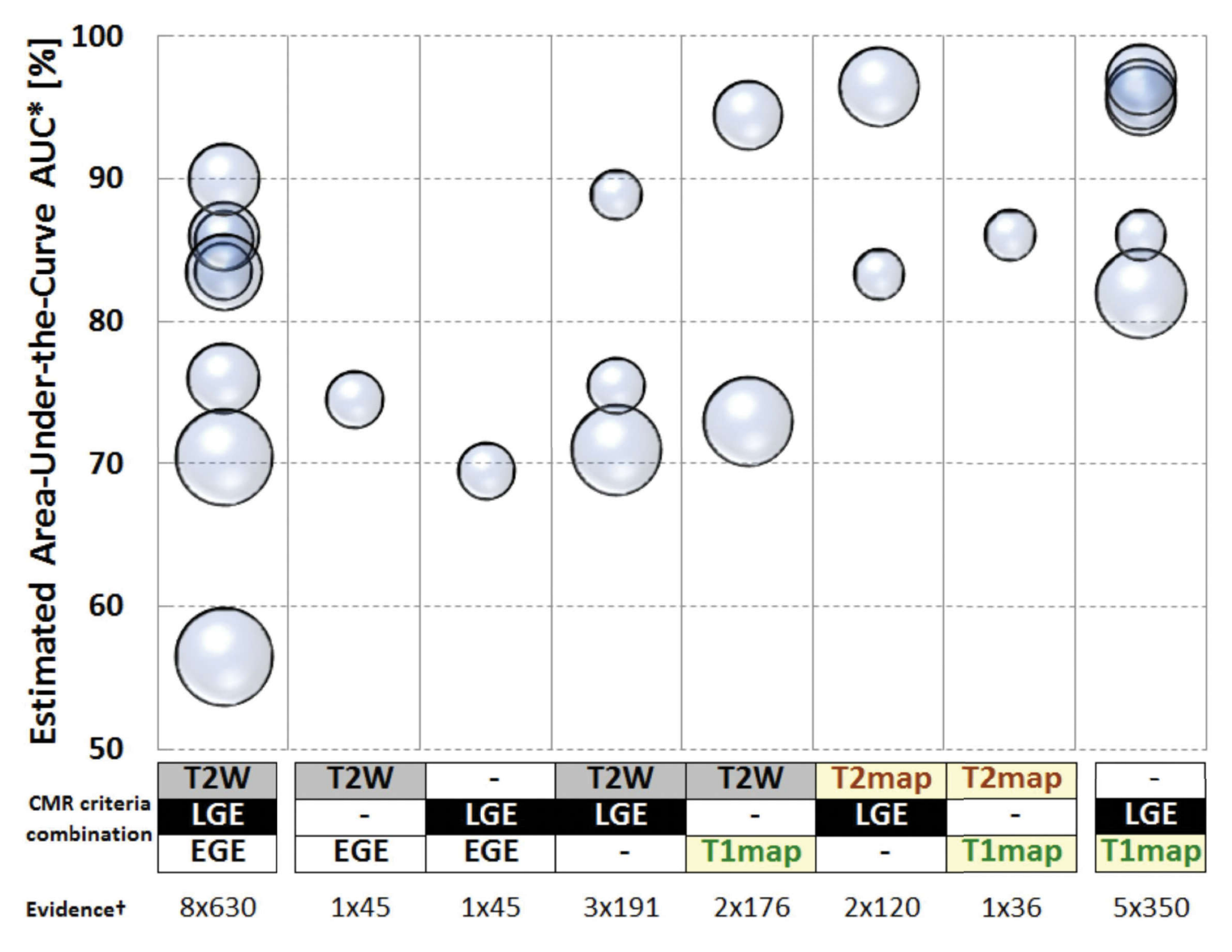
Estimated Area-Under-the-Curve AUC* [%]
100
90
80
70
60
50
CMR criteria combination
T2W
LGE
EGE
T2W
-
EGE
-
LGE
EGE
T2W
LGE
-
T2W
-
LGE
EGE
T2W
-
T1map
T2map
LGE
-
T2map
-
T1map
-
LGE
T1map
Evidence†
8x630
1x45
1x45
3x191
2x176
2x120
1x36
5x350

SUPPLEMENTAL MATERIAL

CMR protocol

While the selection of the CMR protocol components may be subject to specific clinical scenarios, it is recommended that centres use a local standard protocol for all cases in which active inflammation should be either ruled out or confirmed, even in follow-up studies. For patients in whom gadolinium-based contrast agents are not desirable or in certain patients with a very low pre-test likelihood for acute coronary syndrome, a protocol based on cine images and mapping only may be considered in institutions experienced in mapping and have locally validated normal ranges for those techniques. In acute settings, the presence of edema is critical for verifying or refuting the diagnosis of "acute" or "active" myocardial inflammation. Myocardial inflammation may be diffuse or regional. CMR cannot detect regional inflammation which is not present in the slice(s) examined. It is therefore necessary to obtain full coverage of the myocardium with at least one sequence from each of the T1 and T2 categories, in order not to lose sensitivity to detect regional involvement. In the absence of any regional findings, sequences capable of detecting diffuse disease (T2 mapping, T2 ratio, T1 mapping, ECV) should be sampled, usually to obtain an average of measurements from at least three locations. Very mild changes or mild ongoing inflammation and edema may not be detectable during later stages.

Unless otherwise noted, all sequences are acquired as breath-holds in a comfortable and enable longer breath-holds, preferably end-expiratory, position (as patients will hold their breath more reproducibly); for some subjects, breath-holds in the end-inspiratory position may be more comfortable; free-breathing protocols with navigator gating may be used if necessary. All sequences are acquired using a cardiac phased array surface coil, except where noted below. As for all CMR studies, a robust ECG signal that assures accurate gating with zero tolerance for

false triggering, is mandatory; degradation of image quality from any cause will compromise the quantitative accuracy of all subsequent measurements. A high-fidelity respiratory wave form to monitor the quality of the breath-holds and the pattern during free breathing, is highly valuable for making scan adjustments and giving feed-back to the patient. Take full advantage of the patient's breath-hold capacity (above 15-20 seconds in some patients) to increase slice coverage / breath-hold, permit use of lower acceleration factors, or limit the width of the acquisition window in the cardiac cycle (for less motion-related blurring). Consider a brief period of hyperventilation in patients with difficulties breath-holding. Late- or end-systolic acquisition is recommended for all fast spin-echo and late gadolinium enhancement sequences (inversion time permitting) in case of fast heart rates or arrhythmias (frequent premature beats or atrial fibrillation), to minimize arrhythmia-related image degradation.

Some of the common scan parameters are suggested below, but may be tailored. For more specific recommendations on the clinical use of parametric mapping, its set-up and applications, we refer to the recently published Society for Cardiovascular Magnetic Resonance Mapping Consensus Statement (1) .

i.) Multi-slice un-gated SSFP sagittal localizers covering the width of the mediastinum. The rectangular Field of View (FOV) is large (38 cm) in the frequency-encoding superior – inferior direction to verify that the heart is reasonably centered within the sensitive region of the surface coils, with re-positioning of the patient as indicated. Slice thickness / gap = 7.5 / 1.5 mm. Y-lines (Y-res) 160. Bandwidth (Bw) 125 kHz. Breath-hold time = 8 sec (16 slices).

ii.) Calibration scan for SENSE acceleration and image signal intensity correction, if indicated.

Use manufacturer recommended scan parameters. Breath-hold = 13 sec.

iii.) Multi-slice SSFP axial localizers, covering the range from just below the cardiac apex, to the aortic arch vessel origins. The field of view is shifted left-ward to include the left lateral chest wall to survey availability of skeletal muscle reference regions of interest. Frequency-encoding left – right, FOV +/- 30 cm with anterior and posterior air-gap to avoid acceleration-related artifact, thickness 7.5 mm skip 1.5 mm, Y-res = 192, Bw = 125 kHz, acceleration = 2. In un-gated mode 30 slices = 12 secs; this stack can alternatively be acquired with image acquisition gated to diastole (1 slice / heart beat) which will likely require that the scan range be more limited to the just heart (as the heart-rate allows), to fit within a breath-hold.

iv.) Left ventricular long axis SSFP cines: This is a good opportunity to advance the patient to test his / her capacity for a longer breath-hold, by acquiring 3 slices during a single breath-hold for better coverage and more complete evaluation. Frequency encoding superior – inferior, FOV +/- 35 cm, thickness 7.5 mm skip 1.5 mm, Y-res = 160 or 176, views per segment 16 to 18, Bw = 125 kHz, acceleration = 2. Breath-hold = 20 secs at heart rate = 64 bpm.

v.) Multi-slice single-shot SSFP localizers in long axis view during free breathing. Copy prescription from iv.) above and extend coverage across the full width of the left ventricle, to capture the position of the LV during quiet respiration. These images will be used to correctly position the stack of non-breath-hold T1 spin echo images for the EGE ratio, in the superior-inferior direction. Scan parameters are the same as for the axial localizers above (with field-of-view adjusted), and gated for diastolic acquisition. Time < 10 sec, no breath-hold instructions.

vi.) Horizontal long axis SSFP cines: Same scan parameters as iv.) above, but field of view can be reduced. 3 slices in one breath-hold.

For tissue characterization techniques, whole LV coverage will increase the diagnostic yield of detecting regions of myocardial inflammation, although this will lengthen scan time. At least 3 short-axis slices covering the LV should be obtained, recognizing that incomplete coverage will increase the potential of missing areas of myocardial inflammation.

vii.) Fast (turbo) spin echo T2-w short axis images, for detection of regional myocardial edema, and pericardial edema if there is associated pericarditis. Acquire using the cardiac phased array coil for improved signal-to-noise. Acquire with fat suppression (chemical fat sat or SPAIR). Use of a dual-echo technique (TE1 approximately 65 ms, TE2 in 120 – 130 ms range) yields one image with better signal-to-noise, and one image with better T2-w contrast for improved chance of visualizing regional T2 hyperintensity and confirming equivocal findings. The dual-echo technique will lengthen the scan and breath-hold time by approximately 50%, but is still within reach for most patients. Echo train length (turbo factor) = 26 or 28, Y-res = 192, slice thickness 9 - 10 mm skip 1 - 2 mm, FOV to suit, Bw = 62.5 kHz, acceleration factor 1.5 to 2.0, triggered q2 R-R intervals. The timing of the acquisition in the cardiac cycle is during the mid-diastolic diastasis period, except at faster heart rates where this mid-diastolic quiet period disappears, or in the presence of arrhythmias (PACs, PVCs, atrial fibrillation). In these cases, the acquisition window is shifted into late systole so that data readout ends immediately before the onset of isovolumic relaxation, thereby minimizing arrhythmia-related motion degradation. An inspection of the previously acquired paraseptal long

axis and / or horizontal long axis cines will be useful to define this timing accurately may be useful. Apply a surface coil intensity correction if a surface coil is used.

viii.) Fast spin echo T2 images for measuring global myocardial-to-skeletal muscle T2 ratio. Obtain (typically short-axis) slices that show as much LV myocardium as possible, together with an adequate sample of skeletal muscle. A repeated acquisition using the body coil with a triple-inversion-recovery prep pulse, for uniform sensitivity profile and fat-suppression across the full field of view may be useful. The TE should be selected at 65 ms (for which the ratio has been validated), triggered on every 2nd or, in heart rates above 80 beats/min, every 3rd heart beat to allow for full T2 recovery.

ix.) T2 mapping: At least 3 (ideally whole LV coverage) short axis slices should be obtained to evaluate for diffuse inflammatory changes, to sample the myocardium more adequately, using the average T2 value as a global measure. The slices are commonly prescribed at suitable locations near the beginning, middle and end of the central 1/3 of the left ventricle, in order to minimize volume averaging errors in the basal and apical thirds of the LV due to sloping walls at the base of the ventricle, leading into the LV outflow tract, or in the apical region. Use the T2 mapping sequence available from the vendor pulse sequence library on the scanner, with the scan parameters as selected, tailoring the field-of-view to suit.

x.) Native T1 mapping: Copy the same 3 (ideally whole LV coverage) slice positions as was used for T2 mapping above. Use the T1 mapping sequence and recommended scan parameters which are available from the vendor pulse sequence library on the scanner, with normal and threshold T1 values as validated at the local institution, which should be benchmarked against published norms and thresholds for the method, if available.

During image acquisition, mis-triggered heart beats may lead to underestimated T1 values; immediate quality control maps may aid in on-the-spot identification of poor T1-maps, allowing reacquisition to obtain the best quality data for interpretation for diagnosis. Parametric maps will still benefit from proper breath-holds, even if motion-correction (MOCO) algorithms are built in, as MOCO can only correct for in-plane but not through-plane motion. Volume-selective B0 shimming focused on the heart is essential at 3 T.

xi.) Pre- and post-gadolinium T1 spin echo images for Early Gadolinium Enhancement Ratio: A multi-slice stack of spin-echo images is acquired through the LV myocardium during quiet respiration. Usually an axial stack is preferred; short axis slices can sometimes also be used. The images are acquired sequentially (not interleaved) from inferior to superior, so that the superior border of the LV myocardium is reached at end systole. This way the images to be analyzed will have been acquired during systole when the ventricular motion is less brisk (than during early diastolic rapid filling, for example), the walls are thicker, and premature beats will have much less impact degrading the images. Accurate positioning in the superior-inferior dimension is assured by referencing the paraseptal long axis "single shot" SSFP multi-slice localizer series acquired during quiet respiration (in v.) above). The field-of-view position is verified using the SSFP axial localizer series to make sure available skeletal muscle reference regions in the left lateral chest wall are not cut out. The scan plane may be tipped down slightly towards the apex for better alignment with the long axis of the ventricle and thus less potential volume averaging during later region-of-interest analysis (optional); if overdone this could make the scan plane excessively oblique to the skeletal muscle reference, however. A localized shim volume should be large enough and positioned so as to include both the LV myocardium and the skeletal muscle

reference region. A spatial saturation band is applied towards the right side of the field-of-view to completely cover the atria; this may help to saturate the spins and promote a better black blood effect when the blood flows into the ventricles. The saturation band is double oblique with the edge to be aligned with the end-diastolic position of the atrio-ventricular groove in both the paraseptal long axis and horizontal long axis cines acquired previously, taking care not to encroach on any available skeletal muscle reference region identified in the axial localizer series. The scan is acquired using the body coil, for uniform sensitivity profile across both the myocardium as well as the skeletal muscle. Slice thickness 7.0 mm, gap 1.5 mm, Y-resolution = 128, 4 signal averages. A fast spin echo pulse sequence is used with turbo factor = 2, so that the acquisition fits within approximately a 4-minute time window.

The breathing pattern during the acquisition is important, and the patient is instructed to breathe "shallow, regular, small, little breaths", - the redundancy hopefully making a bigger impression to achieve this result. The patient must also be instructed not to fall asleep, as deep, irregular breaths, snoring and Cheyne-Stokes breathing during sleep will be highly destructive to image quality. A good-quality respiratory wave-form for observing the breathing pattern is very helpful, so that a scan can be stopped early and restarted after further coaching of the patient, if indicated.

The pre-gadolinium baseline scan is inspected to verify that image quality is satisfactory and that adequate skeletal muscle reference regions are available for analysis. A standard dose (0.1 mmol/kg for a standard gadolinium agent) followed by 25cc of flush solution is then administered IV (typically at 1.5 or 2 cc/sec), preferably by remote infusion so the patient does not need to be removed from the magnet, and the post-gadolinium scan can be started as soon as the bolus has been delivered. The goal is to

complete the acquisition within 4 minutes of having delivered the gadolinium bolus (if the heart rate is slow, this target may be exceeded slightly). It is safest to rerun the baseline scan within the same series using identical scan parameters, and to not repeat the pre-scan in order to be sure that all the pre-scan settings remain unchanged, for the calculated myocardial and skeletal muscle enhancement values to be valid. At the completion of the post-gadolinium series a 2nd dose of 0.1 mmol/kg of gadolinium is administered (for a total dose of 0.2 mmol/kg, eGFR permitting) after having made sure the patient continues to feel fine (no allergic symptoms).

During image analysis, regions of interest are traced around the entire myocardium in (at least) 3 slices located centrally in the (oblique) axial spin-echo image stack through the LV, avoiding slices located further superiorly or closer to the diaphragm where the myocardium is more oblique to the scan plane, which increases the potential for volume averaging in signal from outside the myocardium. The contours are traced to capture a solid core of myocardium only, taking care to exclude contamination by bright signal along the endocardial borders (representing gadolinium-enhanced slow-flowing blood along the walls, including the RV side of the septum), or from the overlying epicardial fat layer. The skeletal muscle region of interest is drawn as large as possible in the serratus anterior or latissimus dorsi muscles, while avoiding areas of visible fatty infiltration. Muscles in the left upper arm are best avoided, because signal intensity values here may be corrupted by edge effects close to the periphery of the magnet bore.

xii.) SSFP cine data set for ventricular function. Usually acquired as a short axis cine stack covering the range from the mitral inflow region to the cardiac apex. Alternatively, a data set with multiple radial long axis cines prescribed using the previously acquired paraseptal and horizontal long axis cines and T2 short axis views, will provide the most

efficient comprehensive evaluation of structure and function. Definition of the mitral (and aortic) valve planes is likely to be more accurate in long axis compared to short axis cine data sets during post-processing segmentation for volumes and ejection fraction (but right ventricular volumes will not be available). 9 evenly spaced radial slices will sample function at 3 positions centered within each of the 6 AHA segments around the circumference of the left ventricle. The field of view is sized for a tight fit in the paraseptal long axis view (which is approximately the largest cross-section encountered during the rotation), with Y-resolution 192, 176 or 160, views / segment = 18, acceleration factor 2 and slice thickness 7.5 skip 1.5 mm. Whether short axis or radial long axis views are used, the goal is to cover 3 slices / breath-hold.

xiii.) As an option, a high resolution T1 fast spin echo short axis stack can be performed to assess for pericardial pathology, specifically for possible peri-myocarditis; it can also demonstrate regional T1 hyperenhancement in areas of inflammation (one of the T1 criteria). Chemical fat saturation is selected to suppress epicardial and pericardial fat signal and improve contrast for visualizing the gadolinium-enhanced pericardial layers. Slice thickness = 7mm, gap 1.5mm, covering basal and mid-ventricular levels (about 8 slices); in the apical region the sloping walls are too oblique to the short axis scan plane to profile the pericardial layers well. Y-resolution 320, turbo factor 16, acceleration factor 2, Bw 62.5 kHz, TE +/- 10ms, trigger q1 R-R, 2 slices / breath-hold. If the sequences have been set up and are ready by the end of the two free-breathing acquisitions in xi.) above, it may be possible to complete both the cines for function as well as the T1 fast spin echo stack for pericardial morphology, during the delay after gadolinium administration was completed, before starting the late gadolinium enhancement imaging.

xiv.) Cine Inversion Recovery (TI scout), short axis slice at a mid-ventricular level, to obtain a first estimate of the inversion time that will null the signal from normal myocardium. Y-resolution 144, 6 or 8 views / segment, thickness 8 mm, q2 R-R, 20 deg. flip angle, reconstruct 60 phases.

xv.) Late Gadolinium Enhancement (LGE) images: Multiple pulse sequence options are available for this, including SSFP-based "single shot" LGE (most suitable as an initial overview to make sure at least some delayed enhancement information has been captured, or as a "bail-out" option for patients with severe arrhythmias, or who cannot perform adequate breath-holds), free-breathing navigator gated 3D volume acquisition (may become prohibitively time consuming, depending on navigator efficiency, if it is necessary to repeat the sequence with a more optimal inversion time setting), or a 3D breath-hold multi-slab volume (which can permit the inversion time to be updated along the way, and which can cover the ventricle with about ½ the number of breath-holds needed for a 2D multi-slice technique, while limiting the acquisition window duration in the cardiac cycle to minimize motion-related blurring). The diagnostic standard continues to be the sequential breath-hold 2D multi-slice segmented inversion recovery sequence with q2 R-R triggering. Q3 R-R triggering is selected at faster heart-rates (> +/- 80 bpm) to maintain a better signal-to-noise ratio, with small adjustments of views / segment (increase), acceleration factor (increase) and Y-resolution (decrease), as necessary to keep the breath-hold duration in range. Select phase sensitive reconstruction if available, and acquire a mid-ventricular test image with the initial inversion time (TI) setting guided by the TI scout sequence in xv.) above (usually +/- 40 ms longer than the inversion time for the best myocardial nulling in the TI scout). If myocardial nulling is suboptimal, adjust the TI time and repeat the test image as necessary until a satisfactory value is found. The TI time gradually becomes longer

with slower heart rates (or with q2 R-R or q3 R-R triggering instead of q1 R-R) and with lower doses of gadolinium (e.g. with ½-dose gadolinium 0.1 mmol/kg for patients with renal impairment). The optimal TI setting also slowly lengthens over time due to renal excretion during scanning, requiring small adjustments (typically + 20 ms increments) when the nulling of myocardial signal drifts off target while scanning progresses through the slices. Slice thickness 8 mm, Y-resolution 192 or 208, views /segment 14 – 18 range, acceleration factor 1.75. Usually short axis slices are obtained, with additional orthogonal long axis views if necessary, tailored to obtain a better perspective of the lesion extent, or to confirm equivocal findings. Phase-sensitive inversion-recovery techniques (PSIR) are often helpful because they are less sensitive to a suboptimal selection of the inversion time.

xvi.) Post-contrast T1 mapping: Repeat the T1 mapping measurements for the same 3 (or more) slices as in (x.) above, at approximately 15 min after completion of the 2nd gadolinium infusion, for calculation of Extra-Cellular Volume fraction. Hematocrit for the calculation of ECV should be obtained immediately before the scan.

Statistical Methods used for Systematic Data Review

For the purposes of this consensus statement, we collated papers reporting on the diagnostic performance of relevant CMR tissue characterization techniques in the context of acute myocarditis, based on manual searches in PubMed and references lists of identified studies. Our list of included papers (Table 2 in the main paper) largely overlap with a recently published formal literature search and meta-analysis on the topic (Online Appendix in Kotanidis et al. (2))

For comparing the diagnostic performance of various CMR combination methods, direct comparison of area-under-the-curve (AUC) for different combinations would have been ideal; however, AUC does not apply to binary criteria combinations in published CMR studies. Thus, to allow meaningful comparison of various CMR combination methods, we chose the estimated area-under-the-curve (AUC*), defined as the average of the sensitivity (SN) + specificity (SP) reported for each combination in each selected reference, i.e. (SN + SP)/2. This index is proportional to the Youden index (3) but conveniently resides on the same scale, and may be interpreted as an estimate of the AUC (AUC*). In our opinion, the arithmetic mean AUC* is less sensitive to the chosen balance between sensitivity and specificity, when compared to the use of harmonic and geometric means, such as F or G scores (4,5). The advantage of this approach is that comparisons of diagnostic performance are reduced to a single variable rather than two independent dimensions (2). The limitation remains that AUC* only reduces, but does not ultimately remove, bias arising from any preferential selection of diagnostic thresholds along the ROC curve.

Effect size is described by the mean/SD weighted by the group study size with non-parametric measures converted as mean (SD)=Median (0.74*IQR). Effect sizes can be calculated and compared only for non-binary components of any combination criteria. Criteria such as LGE,

and the Original Lake Louise Criteria I, do not have corresponding effect sizes, thus their diagnostic performance is inferred from AUC* (Supplemental Figure 2, below).

For the purpose of conducting the meta-analysis of the diagnostic performance of CMR criteria in detecting myocarditis based on currently available published data, standard error (SE) of the AUC* was calculated using the formula proposed by Hanley & McNeil (6). The meta-analysis was performed in Medcalc (www.medcalc.org, version 18.5). A random effects model was applied. To make the meta-analysis possible, one occurrence of ROC*=100% was replaced by 99.9% (diagnostic performance of T2W imaging in (7)).

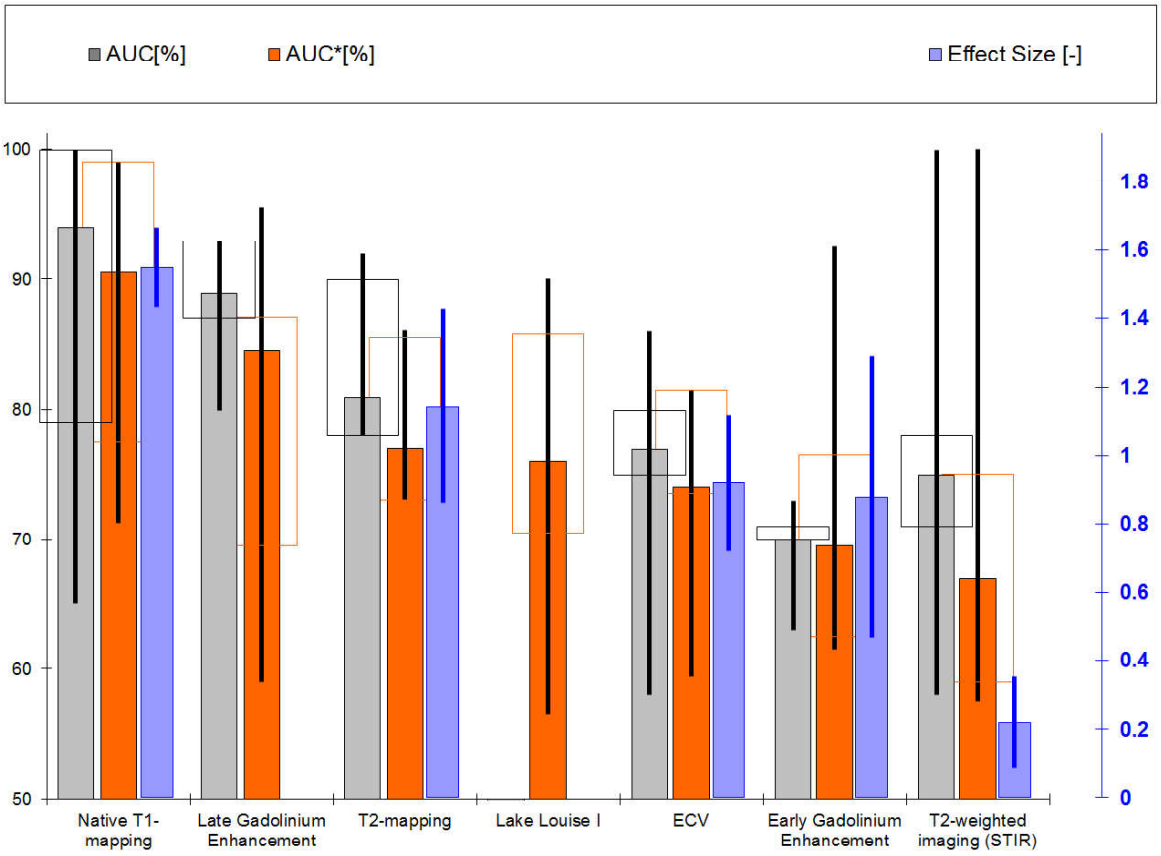

Supplemental Figure 2. Summary of published estimates for the diagnostic performance of CMR methods for detection of acute myocardial inflammation. The criteria are sorted in order of decreasing median "estimated area-under-the-curve" (AUC*, orange bar). AUC* permits the assessment of combination CMR criteria, such as the Original Lake Louise Criteria I, for which the actual area-under-the-curve (AUC; grey bar) is reported in published studies. Effect sizes can be calculated and compared only for non-binary CMR methods; thus, criteria such as LGE, and the Original Lake Louise Criteria which contain LGE as a component, do not have corresponding effect sizes. Bar graphs, open box and whiskers correspond to the median, IQR and the 95% CI range of reported literature values, respectively. Effect size is described by the mean/SD weighted by the group study size with non-parametric measures converted as mean (SD)=Median (0.74*IQR).

Supplemental Table 6. Summary of the meta analysis of the observed AUC* between CMR biomarkers and their combinations. A random effects model was applied. Note that the results need to be interpreted with caution due to high heterogeneity within the underlying data as shown in the last two columns.

CMR Criteria	No. of studies (n)	AUC*	Standard error of AUC*	95%CI	Heterogeneity	Inconsistency (I^2)
LL1	8	0.785	0.040	0.707 to 0.862	p = 0.0004	0.738
T2W + EGE	1	0.745	-	-	-	-
LGE + EGE	1	0.695	-	-	-	-
T2W + LGE	3	0.767	0.054	0.662 to 0.872	p = 0.2284	0.323
T2W + T1map	2	0.836	0.076	0.687 to 0.985	p = 0.0038	0.881
T2 map + LGE	2	0.928	0.059	0.811 to 1.000	p = 0.2033	0.382
T2 map + T1 map	1	0.861	-	-	-	-
T1 map + LGE	5	0.917	0.030	0.858 to 0.977	p = 0.1142	0.463
T2W	13	0.726	0.031	0.666 to 0.787	p = 0.0028	0.600
EGE	10	0.727	0.029	0.670 to 0.783	p = 0.0646	0.441
LGE	13	0.778	0.033	0.713 to 0.844	p < 0.0001	0.742
T1map	9	0.871	0.029	0.814 to 0.928	p = 0.0080	0.614
T2map	6	0.795	0.026	0.744 to 0.845	p = 0.6166	0.000
ECV	7	0.75	0.024	0.703 to 0.797	p = 0.7066	0.000
ALL CMR	80	0.79	0.013	0.765 to 0.815	p < 0.0001	0.697

Note: "-" indicate missing data for single-study CMR criteria where meta-analysis was not performed, with the single AUC* of that study quoted. Red indicates statistically significant Cochran's measure of heterogeneity at $p<0.1$ (8). I^2 is the proportion of observed total variation across studies that is due to real heterogeneity rather than chance. AUC* – "estimated" area-under-the-curve**,** defined as the average of the sensitivity (SN) + specificity (SP) reported for each combination in published studies, i.e. (SN + SP)/2.

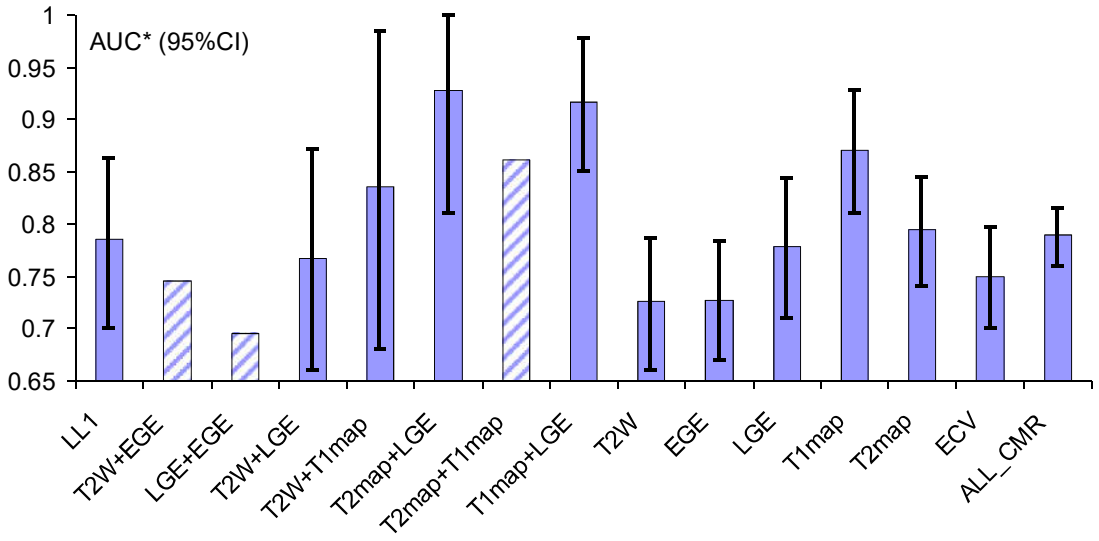

Supplemental Figure 3. Summary of the meta-analysis of the estimated area-under-the-curve (AUC*) between CMR criteria and their combinations. Striped bars without confidence interval (CI) whiskers are single study values. Note that the results should be interpreted with caution due to the high degree of heterogeneity in currently available data in published reports (see also Supplemental Table 6) and Figure 1 in the main manuscript.

References (Supplemental Material)

1. Messroghli DR, Moon JC, Ferreira VM, et al. Clinical recommendations for cardiovascular magnetic resonance mapping of T1, T2, T2* and extracellular volume: A consensus statement by the Society for Cardiovascular Magnetic Resonance (SCMR) endorsed by the European Association for Cardiovascular Imaging (EACVI). J Cardiovasc Magn Reson 2017;19:42–24

2. Kotanidis CP, Bazmpani M, Haidich A, Karvounis C, Antoniades C, Karamitsos TD. Diagnostic Accuracy of Cardiovascular Magnetic Resonance in Acute Myocarditis: A Systematic Review and Meta-Analysis.JACC: Cardiovascular Imaging 2018; Feb 9; doi.org/10.1016/j.jcmg.2017.12.008.

3. Youden, W.J. (1950). "Index for rating diagnostic tests". Cancer. 3: 32–35.

4. Powers DMW. Evaluation: From Precision, Recall and F-Measure to ROC, Informedness, Maekedness & Correlation. Journal of Machine Learning Technologies 2011;2:37–63.

5. Fowlkes EB, Mallows CL. A Method for Comparing Two Hierarchical Clusterings. Journal of the American Statistical Association 1983;78:553–569.

6. Hanley JA and McNeil BJ. The meaning and use of the area under a receiver operating characteristic (ROC) curve. Radiology. 1982 Apr;143(1):29-36.

7. Knobelsdorff-Brenkenhoff von F, Schüler J, Doganguzel S, et al. Detection and Monitoring of Acute Myocarditis Applying Quantitative Cardiovascular Magnetic Resonance. Circ Cardiovasc Imaging 2017; Feb;10 (2).

8. Higgins JP, Thompson SG, Deeks JJ, Altman DG (2003) Measuring inconsistency in meta-analyses. BMJ 327:557-560.

CMR Criterion (Individual)	Study	Study design	Sample size (n)	Patient (n)	Controls (n)	AUC (%)	SN (%)	SP (%)	Accuracy	PPV (%)	NPV (%)	AUC*=(SN+SP)/2	F1	Control mean	Control SD	Patient mean	Patient SD	Effect size	Analysis	Threshold	Population	Validation	Time from presentation to CMR (days)	Sequence characteristics
T2-weighted imaging (STIR)	[illegible]	[illegible]	[illegible]	[illegible]	[illegible]		[illegible]	[illegible]	[illegible]	[illegible]	[illegible]	[illegible]	[illegible]						[illegible]	[illegible]	[illegible]	[illegible]	[illegible]	[illegible]
T2-weighted imaging (STIR)	[illegible]	[illegible]	[illegible]	[illegible]	[illegible]		[illegible]	[illegible]	[illegible]	[illegible]	[illegible]	[illegible]	[illegible]						[illegible]	[illegible]	[illegible]	[illegible]	[illegible]	[illegible]
T2-weighted imaging (STIR)	[illegible]	[illegible]	[illegible]	[illegible]	[illegible]		[illegible]	[illegible]	[illegible]	[illegible]	[illegible]	[illegible]	[illegible]	[illegible]	[illegible]	[illegible]	[illegible]	[illegible]	[illegible]	[illegible]	[illegible]	[illegible]	[illegible]	[illegible]
T2-weighted imaging (STIR)	[illegible]	[illegible]	[illegible]	[illegible]	[illegible]		[illegible]	[illegible]	[illegible]	[illegible]	[illegible]	[illegible]	[illegible]	[illegible]	[illegible]	[illegible]	[illegible]	[illegible]	[illegible]	[illegible]	[illegible]	[illegible]	[illegible]	[illegible]
T2-weighted imaging (STIR)	[illegible]	[illegible]	[illegible]	[illegible]	[illegible]		[illegible]	[illegible]	[illegible]	[illegible]	[illegible]	[illegible]	[illegible]						[illegible]	[illegible]	[illegible]	[illegible]	[illegible]	[illegible]
T2-weighted imaging (STIR)	[illegible]	[illegible]	[illegible]	[illegible]	[illegible]		[illegible]	[illegible]	[illegible]	[illegible]	[illegible]	[illegible]	[illegible]						[illegible]	[illegible]	[illegible]	[illegible]	[illegible]	[illegible]
T2-weighted imaging (STIR)	[illegible]	[illegible]	[illegible]	[illegible]	[illegible]		[illegible]												[illegible]	[illegible]	[illegible]	[illegible]	[illegible]	[illegible]
T2-weighted imaging (STIR)	[illegible]	[illegible]	[illegible]	[illegible]	[illegible]	[illegible]	[illegible]	[illegible]	[illegible]	[illegible]	[illegible]	[illegible]	[illegible]	[illegible]	[illegible]	[illegible]	[illegible]	[illegible]	[illegible]	[illegible]	[illegible]	[illegible]	[illegible]	[illegible]
T2-weighted imaging (STIR)	[illegible]	[illegible]	[illegible]	[illegible]	[illegible]	[illegible]	[illegible]	[illegible]	[illegible]	[illegible]	[illegible]	[illegible]	[illegible]	[illegible]	[illegible]	[illegible]	[illegible]	[illegible]	[illegible]	[illegible]	[illegible]	[illegible]	[illegible]	[illegible]
T2-weighted imaging (STIR)	[illegible]	[illegible]	[illegible]	[illegible]	[illegible]	[illegible]	[illegible]	[illegible]	[illegible]	[illegible]	[illegible]	[illegible]	[illegible]	[illegible]	[illegible]	[illegible]	[illegible]	[illegible]	[illegible]	[illegible]	[illegible]	[illegible]	[illegible]	[illegible]
T2-weighted imaging (STIR)	[illegible]	[illegible]	[illegible]	[illegible]	[illegible]	[illegible]	[illegible]	[illegible]	[illegible]	[illegible]	[illegible]	[illegible]	[illegible]	[illegible]	[illegible]	[illegible]	[illegible]	[illegible]	[illegible]	[illegible]	[illegible]	[illegible]	[illegible]	[illegible]
T2-weighted imaging (STIR)	[illegible]	[illegible]	[illegible]	[illegible]	[illegible]	[illegible]	[illegible]	[illegible]	[illegible]	[illegible]	[illegible]	[illegible]	[illegible]						[illegible]	[illegible]	[illegible]	[illegible]	[illegible]	[illegible]
T2-weighted imaging (STIR)	[illegible]	[illegible]	[illegible]	[illegible]	[illegible]	[illegible]	[illegible]	[illegible]	[illegible]	[illegible]	[illegible]	[illegible]	[illegible]	[illegible]	[illegible]	[illegible]	[illegible]	[illegible]	[illegible]	[illegible]	[illegible]	[illegible]	[illegible]	[illegible]
T2-weighted imaging (STIR)	[illegible]	[illegible]	[illegible]	[illegible]	[illegible]									[illegible]	[illegible]	[illegible]	[illegible]	[illegible]	[illegible]	[illegible]	[illegible]	[illegible]	[illegible]	[illegible]
T2-weighted imaging (STIR)	[illegible]	[illegible]		[illegible]	[illegible]									[illegible]	[illegible]	[illegible]	[illegible]	[illegible]	[illegible]	[illegible]	[illegible]	[illegible]	[illegible]	[illegible]
T2-weighted imaging (STIR)	[illegible]	[illegible]	[illegible]	[illegible]	[illegible]	[illegible]	[illegible]	[illegible]	[illegible]	[illegible]	[illegible]	[illegible]	[illegible]	[illegible]	[illegible]	[illegible]	[illegible]	[illegible]	[illegible]	[illegible]	[illegible]	[illegible]	[illegible]	[illegible]
Early Gadolinium Enhancement	[illegible]	[illegible]	[illegible]	[illegible]	[illegible]		84	89	86	89	84	[illegible]	[illegible]	2.5	0.871779789	4.7	1.307669683	[illegible]	[illegible]		[illegible]	[illegible]	[illegible]	[illegible]
Early Gadolinium Enhancement	[illegible]	[illegible]	[illegible]	[illegible]	[illegible]		85	100	89	100	70	[illegible]	[illegible]	0.29	0.138636215	0.56	0.084664042	[illegible]	[illegible]	45%	[illegible]	[illegible]	[illegible]	[illegible]
Early Gadolinium Enhancement	[illegible]	[illegible]	[illegible]	[illegible]	[illegible]		[illegible]	[illegible]	[illegible]	[illegible]	[illegible]	[illegible]	[illegible]	[illegible]	[illegible]	[illegible]	[illegible]	[illegible]	[illegible]	[illegible]	[illegible]	[illegible]	[illegible]	[illegible]
Early Gadolinium Enhancement	[illegible]	[illegible]	[illegible]	[illegible]	[illegible]		[illegible]	[illegible]	[illegible]	[illegible]	[illegible]	[illegible]	[illegible]	[illegible]	[illegible]	[illegible]	[illegible]	[illegible]	[illegible]	[illegible]	[illegible]	[illegible]	[illegible]	[illegible]
Early Gadolinium Enhancement	[illegible]	[illegible]	[illegible]	[illegible]	[illegible]		[illegible]	[illegible]	[illegible]	[illegible]	[illegible]	[illegible]	[illegible]						[illegible]	[illegible]	[illegible]	[illegible]	[illegible]	[illegible]
Early Gadolinium Enhancement	[illegible]	[illegible]	[illegible]	[illegible]	[illegible]		[illegible]	[illegible]	[illegible]	[illegible]	[illegible]	[illegible]	[illegible]	[illegible]	[illegible]	[illegible]	[illegible]	[illegible]	[illegible]	[illegible]	[illegible]	[illegible]	[illegible]	[illegible]
Early Gadolinium Enhancement	[illegible]	[illegible]	[illegible]	[illegible]	[illegible]		[illegible]												[illegible]	[illegible]	[illegible]	[illegible]	[illegible]	[illegible]
Early Gadolinium Enhancement	[illegible]	[illegible]	[illegible]	[illegible]	[illegible]	[illegible]	[illegible]	[illegible]	[illegible]	[illegible]	[illegible]	[illegible]	[illegible]	[illegible]	[illegible]	[illegible]	[illegible]	[illegible]	[illegible]	[illegible]	[illegible]	[illegible]	[illegible]	[illegible]
Early Gadolinium Enhancement	[illegible]	[illegible]	[illegible]	[illegible]	[illegible]	[illegible]	[illegible]	[illegible]	[illegible]	[illegible]	[illegible]	[illegible]	[illegible]	[illegible]	[illegible]	[illegible]	[illegible]	[illegible]	[illegible]	[illegible]	[illegible]	[illegible]	[illegible]	[illegible]
Early Gadolinium Enhancement	[illegible]	[illegible]	[illegible]	[illegible]	[illegible]	[illegible]	[illegible]	[illegible]	[illegible]	[illegible]	[illegible]	[illegible]	[illegible]						[illegible]	[illegible]	[illegible]	[illegible]	[illegible]	[illegible]
Early Gadolinium Enhancement	[illegible]	[illegible]	[illegible]	[illegible]	[illegible]	[illegible]	[illegible]	[illegible]	[illegible]	[illegible]	[illegible]	[illegible]	[illegible]	[illegible]	[illegible]	[illegible]	[illegible]	[illegible]	[illegible]	[illegible]	[illegible]	[illegible]	[illegible]	[illegible]
Early Gadolinium Enhancement	[illegible]	[illegible]	[illegible]	[illegible]	[illegible]									[illegible]	[illegible]	[illegible]	[illegible]	[illegible]	[illegible]	[illegible]	[illegible]	[illegible]	[illegible]	[illegible]
Early Gadolinium Enhancement	[illegible]	[illegible]	[illegible]	[illegible]	[illegible]									[illegible]	[illegible]	[illegible]	[illegible]	[illegible]	[illegible]	[illegible]	[illegible]	[illegible]	[illegible]	[illegible]
Late Gadolinium Enhancement	[illegible]	[illegible]	[illegible]	[illegible]	[illegible]		[illegible]	[illegible]	[illegible]	[illegible]	[illegible]	[illegible]	[illegible]						[illegible]	[illegible]	[illegible]	[illegible]	[illegible]	[illegible]
Late Gadolinium Enhancement	[illegible]	[illegible]	[illegible]	[illegible]	[illegible]		[illegible]	[illegible]	[illegible]	[illegible]	[illegible]	[illegible]	[illegible]						[illegible]	[illegible]	[illegible]	[illegible]	[illegible]	[illegible]
Late Gadolinium Enhancement	[illegible]	[illegible]	[illegible]	[illegible]	[illegible]		[illegible]	[illegible]	[illegible]	[illegible]	[illegible]	[illegible]	[illegible]						[illegible]	[illegible]	[illegible]	[illegible]	[illegible]	[illegible]
Late Gadolinium Enhancement	[illegible]	[illegible]	[illegible]	[illegible]	[illegible]		[illegible]	[illegible]	[illegible]	[illegible]	[illegible]	[illegible]	[illegible]						[illegible]	[illegible]	[illegible]	[illegible]	[illegible]	[illegible]
Late Gadolinium Enhancement	[illegible]	[illegible]	[illegible]	[illegible]	[illegible]		[illegible]	[illegible]	[illegible]	[illegible]	[illegible]	[illegible]	[illegible]						[illegible]	[illegible]	[illegible]	[illegible]	[illegible]	[illegible]
Late Gadolinium Enhancement	[illegible]	[illegible]	[illegible]	[illegible]	[illegible]		[illegible]	[illegible]	[illegible]	[illegible]	[illegible]	[illegible]	[illegible]						[illegible]	[illegible]	[illegible]	[illegible]	[illegible]	[illegible]
Late Gadolinium Enhancement	[illegible]	[illegible]	[illegible]	[illegible]	[illegible]		[illegible]	[illegible]	[illegible]	[illegible]	[illegible]	[illegible]	[illegible]						[illegible]	[illegible]	[illegible]	[illegible]	[illegible]	[illegible]
Late Gadolinium Enhancement	[illegible]	[illegible]	[illegible]	[illegible]	[illegible]		[illegible]												[illegible]	[illegible]	[illegible]	[illegible]	[illegible]	[illegible]
Late Gadolinium Enhancement	[illegible]	[illegible]	[illegible]	[illegible]	[illegible]	[illegible]	[illegible]	[illegible]	[illegible]	[illegible]	[illegible]	[illegible]	[illegible]						[illegible]	[illegible]	[illegible]	[illegible]	[illegible]	[illegible]
Late Gadolinium Enhancement	[illegible]	[illegible]	[illegible]	[illegible]	[illegible]	[illegible]	[illegible]	[illegible]	[illegible]	[illegible]	[illegible]	[illegible]	[illegible]						[illegible]	[illegible]	[illegible]	[illegible]	[illegible]	[illegible]
Late Gadolinium Enhancement	[illegible]	[illegible]	[illegible]	[illegible]	[illegible]	[illegible]	[illegible]	[illegible]	[illegible]	[illegible]	[illegible]	[illegible]	[illegible]						[illegible]	[illegible]	[illegible]	[illegible]	[illegible]	[illegible]
Late Gadolinium Enhancement	[illegible]	[illegible]	[illegible]	[illegible]	[illegible]	[illegible]	[illegible]	[illegible]	[illegible]	[illegible]	[illegible]	[illegible]	[illegible]						[illegible]	[illegible]	[illegible]	[illegible]	[illegible]	[illegible]
Late Gadolinium Enhancement	[illegible]	[illegible]	[illegible]	[illegible]	[illegible]	[illegible]	[illegible]	[illegible]	[illegible]	[illegible]	[illegible]	[illegible]	[illegible]						[illegible]	[illegible]	[illegible]	[illegible]	[illegible]	[illegible]
Late Gadolinium Enhancement	[illegible]	[illegible]	[illegible]	[illegible]	[illegible]	[illegible]	[illegible]	[illegible]	[illegible]	[illegible]	[illegible]	[illegible]	[illegible]						[illegible]	[illegible]	[illegible]	[illegible]	[illegible]	[illegible]
Late Gadolinium Enhancement	[illegible]	[illegible]	[illegible]	[illegible]	[illegible]	[illegible]	[illegible]	[illegible]	[illegible]	[illegible]	[illegible]	[illegible]	[illegible]						[illegible]	[illegible]	[illegible]	[illegible]	[illegible]	[illegible]
Late Gadolinium Enhancement	[illegible]	[illegible]	[illegible]	[illegible]	[illegible]														[illegible]	[illegible]	[illegible]	[illegible]	[illegible]	[illegible]
Late Gadolinium Enhancement	[illegible]	[illegible]	[illegible]	[illegible]	[illegible]														[illegible]	[illegible]	[illegible]	[illegible]	[illegible]	[illegible]
Late Gadolinium Enhancement	[illegible]	[illegible]	[illegible]	[illegible]	[illegible]	[illegible]	[illegible]	[illegible]	[illegible]	[illegible]	[illegible]	[illegible]	[illegible]						[illegible]	[illegible]	[illegible]	[illegible]	[illegible]	[illegible]
Native T1-mapping	[illegible]	[illegible]	[illegible]	[illegible]	[illegible]	[illegible]	[illegible]	[illegible]	[illegible]	[illegible]	[illegible]	[illegible]	[illegible]	[illegible]	[illegible]	[illegible]	[illegible]	[illegible]	[illegible]	[illegible]	[illegible]	[illegible]	[illegible]	[illegible]
Native T1-mapping	[illegible]	[illegible]	[illegible]	[illegible]	[illegible]	[illegible]	[illegible]	[illegible]	[illegible]	[illegible]	[illegible]	[illegible]	[illegible]	[illegible]	[illegible]	[illegible]	[illegible]	[illegible]	[illegible]	[illegible]	[illegible]	[illegible]	[illegible]	[illegible]
Native T1-mapping	[illegible]	[illegible]	[illegible]	[illegible]	[illegible]	[illegible]	[illegible]	[illegible]	[illegible]	[illegible]	[illegible]	[illegible]	[illegible]	[illegible]	[illegible]	[illegible]	[illegible]	[illegible]	[illegible]	[illegible]	[illegible]	[illegible]	[illegible]	[illegible]
Native T1-mapping	[illegible]	[illegible]	[illegible]	[illegible]	[illegible]	[illegible]	[illegible]	[illegible]	[illegible]	[illegible]	[illegible]	[illegible]	[illegible]	[illegible]	[illegible]	[illegible]	[illegible]	[illegible]	[illegible]	[illegible]	[illegible]	[illegible]	[illegible]	[illegible]
Native T1-mapping	[illegible]	[illegible]	[illegible]	[illegible]	[illegible]	[illegible]	[illegible]	[illegible]	[illegible]	[illegible]	[illegible]	[illegible]	[illegible]	[illegible]	[illegible]	[illegible]	[illegible]	[illegible]	[illegible]	[illegible]	[illegible]	[illegible]	[illegible]	[illegible]
Native T1-mapping	[illegible]	[illegible]	[illegible]	[illegible]	[illegible]	[illegible]	[illegible]	[illegible]	[illegible]	[illegible]	[illegible]	[illegible]	[illegible]	[illegible]	[illegible]	[illegible]	[illegible]	[illegible]	[illegible]	[illegible]	[illegible]	[illegible]	[illegible]	[illegible]
Native T1-mapping	[illegible]	[illegible]	[illegible]	[illegible]	[illegible]	[illegible]	[illegible]	[illegible]	[illegible]	[illegible]	[illegible]	[illegible]	[illegible]	[illegible]	[illegible]	[illegible]	[illegible]	[illegible]	[illegible]	[illegible]	[illegible]	[illegible]	[illegible]	[illegible]
Native T1-mapping	[illegible]	[illegible]	[illegible]	[illegible]	[illegible]	[illegible]	[illegible]	[illegible]	[illegible]	[illegible]	[illegible]	[illegible]	[illegible]	[illegible]	[illegible]	[illegible]	[illegible]	[illegible]	[illegible]	[illegible]	[illegible]	[illegible]	[illegible]	[illegible]
Native T1-mapping	[illegible]	[illegible]	[illegible]	[illegible]	[illegible]	[illegible]								[illegible]	[illegible]	[illegible]	[illegible]	[illegible]	[illegible]		[illegible]	[illegible]	[illegible]	[illegible]
Native T1-mapping	[illegible]	[illegible]	[illegible]	[illegible]	[illegible]	[illegible]	[illegible]	[illegible]	[illegible]	[illegible]	[illegible]	[illegible]	[illegible]	[illegible]	[illegible]	[illegible]	[illegible]	[illegible]	[illegible]	[illegible]	[illegible]	[illegible]	[illegible]	[illegible]
T2-mapping	[illegible]	[illegible]	[illegible]	[illegible]	[illegible]	[illegible]	[illegible]	[illegible]	[illegible]	[illegible]	[illegible]	[illegible]	[illegible]	[illegible]	[illegible]	[illegible]	[illegible]	[illegible]	[illegible]	[illegible]	[illegible]	[illegible]	[illegible]	[illegible]

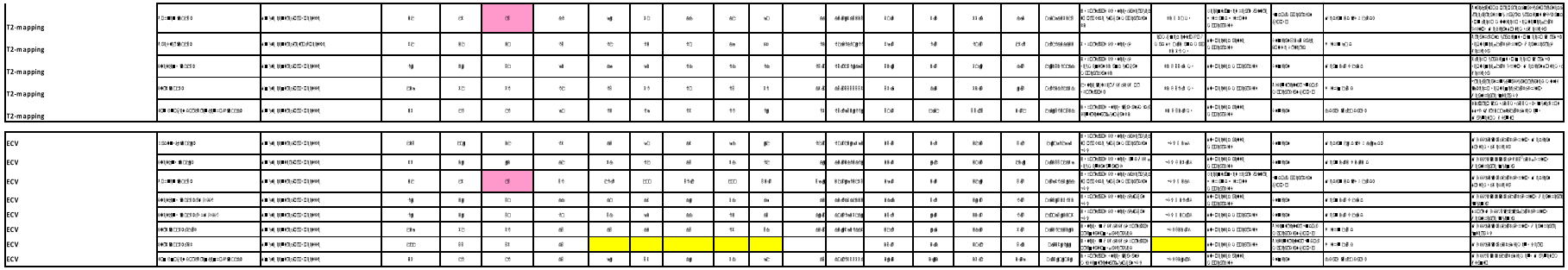

Supplemental table 7 Published reports on the diagnostic accuracy of CMR in suspected myocarditis

CMR Criteria (Combinations)	Study	N-TOTAL	Patient	Controls	SN (%)	SP (%)	Accuracy	PPV (%)	NPV (%)	AUC*
Lake Louise I	Abdel-Aty (2005)	48	25	23	76	95.5	85			85.75
Lake Louise I	Chu (2013)	45	35	10	77	90	53	80	96	83.5
Lake Louise I	Luetkens (2014)	66	24	42	92	80	85	79	92	86
Lake Louise I	Lurz (2016)	129	61	68	66	47	59	71	41	56.5
Lake Louise I	Lurz (2012)	70	53	17	81	71	79	90	55	76
Lake Louise I	Radunski (2014)	125	104	21	84	57	79	90	41	70.5
Lake Louise I	Luetkens (2016)	69	24	45	82	98	92	97	89	90
Lake Louise I	Schwab (2015)	78	43	35	67	100	82	100	72	83.5
T2+EGE	Chu (2013)	45	35	10	49	100	60	100	36	74.5
LGE+EGE	Chu (2013)	45	35	10	49	90	58	94	33	69.5
T2W+LGE	Ferreira (2014)	110	60	50	45	97	64	96	51	71
T2W+LGE	von Knobelsdorf-Brenkenhoff (2017)	36	18	18	77.8	100	88.9			88.9
T2W+LGE	Chu (2013)	45	35	10	91	60	67	84	89	75.5
T2W+T1map	Luetkens (2014)	66	24	42	92	97	95	96	95	94.5
T2W+T1map	Ferreira (2014)	110	60	50	48	98	71	97	61	73
T2map+LGE	von Knobelsdorf-Brenkenhoff (2017)	36	18	18	66.7	100	83.3			83.35
T2map+LGE	Luetkens (2016)	84	34	50	97	96	96	100	94	96.5
T2map+T1map	von Knobelsdorf-Brenkenhoff (2017)	36	18	18	77.8	94.4	86.1			86.1
T1map+LGE	Luetkens (2014)	66	24	42	96	95	96	92	98	95.5
T1map+LGE	Luetkens (2016)	69	24	45	94	98	96	94	98	96
T1map+LGE	Luetkens (2016)	69	24	45	100	94	96	92	100	97
T1map+LGE	Ferreira (2014)	110	60	50	67	97	78	98	63	82
T1map+LGE	von Knobelsdorf-Brenkenhoff (2017)	36	18	18	72.2	100	86.1			86.1

Supplemental table 8 Published reports on the diagnostic accuracy of CMR in suspected myocarditis, sorted by used criteria combinations